<u>Reviewer Responses for Referee #1</u>

**1. The authors need to show that the results are robust to changes in model groups. Perhaps 1/3 of the models are very close to a 1:1 line they use to select models. What happens if you change the grouping of models? Does it change the results?**

As a first test of the model groups, we grouped the five models closest to the 1:1 line into a third group (hereafter Group 3) and constructed joint distributions of *CA* for this group (these models are bcc-csm1-1, CMCC-CM, CanESM2, MPI-ESM-MR, and MPI-ESM-LR; 2 Group 1 models and 3 Group 2 models). These models have smaller differences between average winter and summer *CA* compared to other models in their respective groups, thus we wouldn't expect the joint distributions for this group to resemble either Group 1 or Group 2 explicitly. Below is joint distribution for DJF for Group 3, to be compared to Fig. 8 in the paper. The table on the right shows average DJF *CA* for the ensemble, Group 1, Group 2, and Group 3.

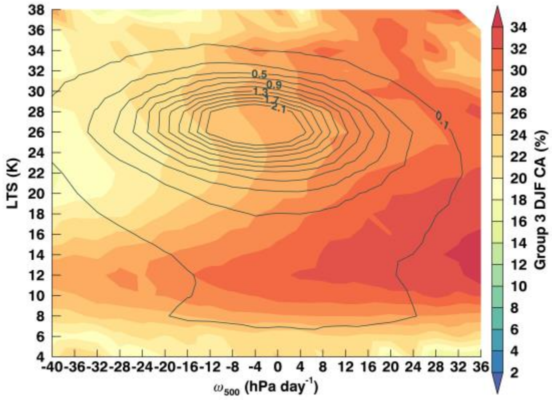


| | Ensemble Mean | Group 1 | Group 2 | Group 3 |
|---|---|---|---|---|
| Avg. DJF *CA* (%) | 21.9% | 28.3% | 18.6% | 25.9% |

The joint distribution for Group 3 contains features present in the joint distributions of both Group 1 and 2 as expected, given that Group 3 is made up of models from each group. For DJF, *CA* increases with increasing $-\omega_{500}$ for low-medium stability (similar to Group 2) but with larger average cloud amount (similar to Group 1). Also similar to Group 1 is the larger *CA* present at high stability and rising motion. The average values of *CA* from the table indicate that Group 1 *CA* > Group 3 *CA* > Group 2 *CA*, as expected for Group 3 given that it contains models from both Group 1 and 2. These examples are given to show that the 1:1 line separating Groups 1 and 2 is a good measure for group selection- if this were not the case then we might expect Group 3 joint distributions to resemble either Group 1 or Group 2. Since Group 3 joint distributions show features from both groups, this is an indication that even the models closest to the 1:1 still represent the low cloud responses of their respective groups. A small change in the grouping has a small effect on the results and does not affect our conclusions.

**2. The authors claim that since their results agree with earlier work, it is fine to use monthly data. That is not sufficient. They are averaging over regimes that may yield very different results, and they need to verify with a single model perhaps that monthly data for joint PDFs for example matches high frequency (daily or higher) data.**

To address this concern, joint distributions of low cloud amount binned by *LTS* and $-\omega_{500}$ were constructed using daily data from IPSL-CM5A-LR for winter (DJF) months and summer (JJA) months for the historical period 1979-2005. Additionally, eqn (1) from the paper was also calculated using the daily data to confirm the validity of monthly data. The CMIP5 archive only had daily vertical cloud amount for one model available, (IPSL-CM5A-LR, a model from Group 1). The results from this model are presented below:

Equation 1: $\overline{LCA} = \sum_{i,j} LCA\left(LTS_i, -\omega_{500,j}\right) * RFO(LTS_i, -\omega_{500,j})$, describing the weighted sum of low cloud amount over $LTS$ and $-\omega_{500}$ from each i,j bin where $LCA\left(LTS_i, -\omega_{500,j}\right)$ is the low cloud amount as a function of $LTS$ and $-\omega_{500}$ and $RFO(LTS_i, -\omega_{500,j})$ is the relative frequency of occurrence of each $LTS$ and $-\omega_{500}$ bin. Applying (1) to daily data from IPSL-CM5A-LR reproduces the domain-averaged LCA with the same accuracy as shown by monthly data in Table 2.

IPSL-CM5A-LR DJF domain-averaged LCA: 25.95%
IPSL-CM5A-LR DJF LCA from Eq. (1): 25.91%
IPSL-CM5A-LR JJA domain-averaged LCA: 16.6%
IPSL-CM5A-LR JJA LCA from Eq. (1): 16.5%

Joint distributions for DJF (left) and JJA (right) low cloud amount binned by $LTS$ and $-\omega_{500}$ are shown below for IPSL-CM5A-LR constructed from daily data (top row) and monthly data (bottom row). Joint distributions for JJA look very similar between the daily and monthly versions: both show a strong gradient in LCA when LTS increases, and the largest LCA for high stability and rising motion. Additionally, the frequency of occurrence of LTS/$-\omega_{500}$ regimes is similar when using either daily or monthly data. One difference between the JJA joint distributions is the presence of highly-stable regimes captured in the daily data (LTS > 25) that are not present in the monthly. However, these highly-stable regimes occur very infrequently (less than the 0.1% frequency of occurrence contour). Differences in DJF joint distributions are larger than for JJA. For low stability (LTS < 12), both daily and monthly distributions show LCA dependent on LTS with little dependence on $-\omega_{500}$. For medium stability (12 < LTS < 26), both show similar amounts of low cloud (particularly in the most frequent regimes) but the daily data shows a slight gradient of larger LCA with increasing $-\omega_{500}$ (this matches with the monthly joint distribution for Group 1 (Fig. 8a in the paper)). The largest differences between daily and monthly data occur for very high stability, as was the case for JJA. Daily joint distributions show the largest LCA for LTS > 34, particularly with rising motion. This is an infrequent regime, however, that the monthly distribution does not capture.

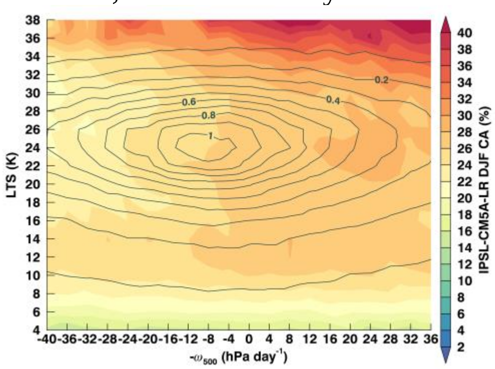


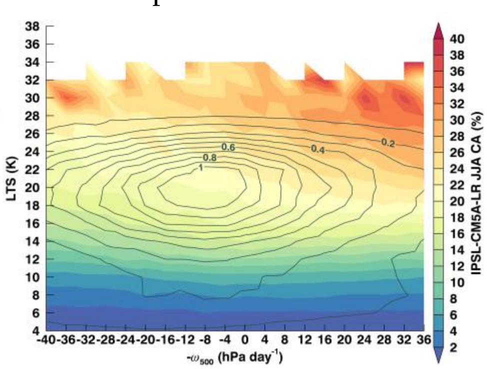

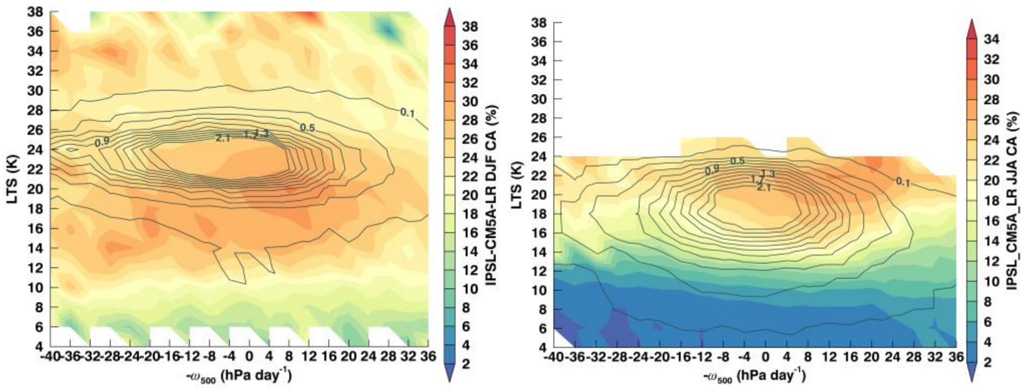


Overall, there are certainly some shortcomings that come with using monthly data, namely the reduced dynamic range. However, the use of monthly data provides useful results especially in most frequent LTS/-$\omega_{500}$ bins. The largest differences between daily and monthly data occurs in the least common LTS/-$\omega_{500}$ bins. The most prevalent regimes in the daily data are also the most frequent regimes in monthly data. Lastly, the availability of daily vertical profile data was a limiting factor in this study, as many models did not provide this output. A sentence was added to the paper (lines 116-118) to reflect the difference between using daily and monthly model output.

**3. The lack of ice fraction is limiting. Analysis shows ice and liquid, with no sense of what the fraction of ice is. This is related to #2 above.**

This is a very helpful suggestion. The production of cloud liquid vs ice is tied to low cloud amount differences, so we have added analysis to the paper and included joint distributions of ice condensate fraction (cloud ice water mixing ratio divided by total cloud condensate mixing ratio) stratified by $T_a$ and *RH* and *LTS* and -$\omega_{500}$ (Figs. 11 and 12). Further, an interesting result of this discussed in the paper and below is that models with a temperature-dependent phase partitioning as opposed to treating cloud ice and liquid as prognostic variables simulate a cloud ice fraction.

**4. The authors need to document models better. There needs to be a table of models with references.**

A table of CMIP5 models (Table 1) and corresponding references has been added, along with a column containing relevant cloud fraction and microphysics schemes for each model.

**5. In addition, it would be particularly useful to group those models which have ice supersaturation and look at their results.**

When adding the suggested model table and compiling relevant microphysics parameterizations for each model, we did not find mention of whether or not a particular model allows ice supersaturation for many of the models (though from our reading, most models do not account for ice supersaturation). We did, however, find a recently published paper that documented the change in Arctic cloud biases in the ECHAM6 atmospheric model when ice supersaturation was allowed (Kretzschmar et al. 2018, published in ACP). The authors found a positive cloud cover bias when compared to CALIPSO due to an overestimation of low-level liquid-containing clouds, and attributed the bias to cloud microphysics. They were able to improve the phase partition between cloud liquid and ice by improving the Wegener-Bergeron-Findeisen process, but the cloud cover bias was only reduced when they allowed for slight supersaturation with respect to ice. Without having the specific information on which of the models in our study have ice supersaturation, the findings in Kretzschmar et al. mirror what we see in our analysis for the models that produce larger low cloud cover. These models have a much larger ice fraction and while one might expect that this leads to more precipitation/removal of ice and hence less cloud cover, other microphysical processes were found to overcompensate for this.

While we did not have complete information on which models allowed supersaturation w.r.t. ice, we do think it is a good suggestion to try grouping the models based on differences in the cloud microphysical parameterizations. Below are joint distributions in DJF of CA (first row), CLW (second row), CLI (third row), and ice condensate fraction (ICF, fourth row) for two new groupings of models: those that calculate both cloud ice and cloud water as prognostic cloud variables, and those that calculate a single mixing ratio of total water and use a temperature dependent partition to determine phase.

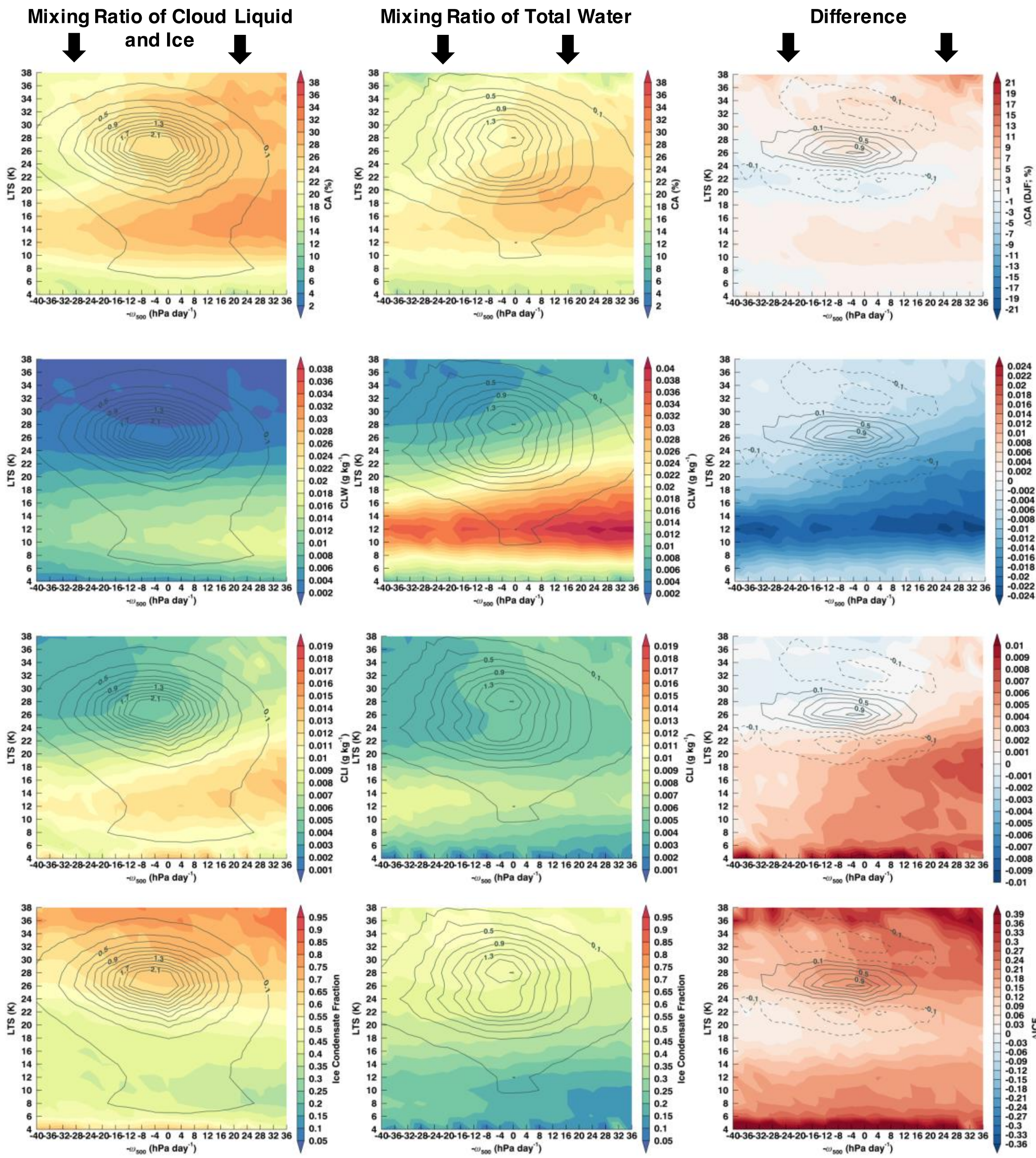


The first thing to notice about the above plots is a visualization of the process described in the previous paragraph whereby the models possessing higher ice fraction/ice mass actually have more cloud cover rather than less. Second, the models that calculate a mixing ratio of total water have less ice and more water than those that calculate both ice and liquid prognostically. For these models, the bounds of the temperature-dependent partitions that determine ice vs. liquid vary. In between these boundary conditions are mixed-phase clouds, and individual model parameterizations determine the growth of ice via the Wegener-Bergeron-Findeisen process or heterogeneous freezing. Since the mixed-phase cloud regime is very common in the Arctic, and that relative concentrations of liquid and ice in the mixed-phase regime vary strongly for different model microphysics parameterizations, it is no surprise that the difference plots for CLW, CLI, and ICF (right column) between these two groupings of models are very large. The difference in cloud fraction between these groupings is smaller than that between the two model groups in our paper, indicating that differences in cloud fraction schemes is part of the answer as to why the models simulate different clouds, but not the whole story.

**6. There is minimal use of observations and comparison with observations in this work. It is hard to tell what is right, would like to see more comparisons against observations, and discussion and conclusions which focus on comparisons with observations. Which group is more like observations?**

We too are interested in knowing which of these models or groups are “correct”. However, this is a difficult question to answer and thoroughly addressing this question is beyond the scope of this paper. Our focus in this study is answering the question ‘Why are the models low cloud amount annual cycle so different?’. A detailed observational comparison study is underway and will be part of a second paper using the same methodology (joint distribution analysis stratifying cloud amount by atmospheric state and cloud influencing factors) applied to observations and CALIPSO-CloudSAT satellite simulator output from available models. We have added a few sentences to the discussion about the observational comparison (Line 376-378).

Moreover, Referee #2 also indicated an interest in how the results might change if we used a different reanalysis dataset. To investigate, we included ERA-Interim in the analysis, giving us one observational dataset (C3M) and 2 reanalysis datasets (MERRA-2 and ERA-Interim) to compare against the model output.

**Specific Comments:**

**Page 5, L164: I’m not sure I would say that the low cloud differences are spatially uniform. Differences seem lower over open water than sea ice for example, and largest differences are over land.**

To address this comment, we calculate the average difference between groups, (G1-G2), for all gridpoints, land gridpoints, and ocean gridpoints for each season (DJF, JJA) and cloud type (low, high). The results are below:

<u>DJF Low Cloud Differences</u>
$\text{G1-G2}_{\text{all gridpoints}}$ = 12.02%
$\text{G1-G2}_{\text{land only}}$ = 11.20%
$\text{G1-G2}_{\text{ocean only}}$ = 12.57%
<u>DJF High Cloud Differences</u>
$\text{G1-G2}_{\text{all gridpoints}}$ = 6.38%
$\text{G1-G2}_{\text{land only}}$ = 7.24%
$\text{G1-G2}_{\text{ocean only}}$ = 5.81%
<u>JJA Low Cloud Differences</u>
$\text{G1-G2}_{\text{all gridpoints}}$ = -7.30%
$\text{G1-G2}_{\text{land only}}$ = -6.56%
$\text{G1-G2}_{\text{ocean only}}$ = -7.78%
<u>JJA High Cloud Differences</u>

$G1\text{-}G2_{\text{all gridpoints}}$ = 3.69%
$G1\text{-}G2_{\text{land only}}$ = 3.34%
$G1\text{-}G2_{\text{ocean only}}$ = 3.92%

From the above, one can see that *CA* differences between Group 1 and Group 2 are very similar whether you use all gridpoints, or ocean and land separately. In order to further quantify the effect of surface type, we have calculated the 95% confidence intervals for the difference in G1-G2 between land gridpoints vs all gridpoints and ocean gridpoints vs all gridpoints.

Results are below:
<u>DJF Low Cloud Differences</u>
$G1\text{-}G2_{\text{land only}}$ - $G1\text{-}G2_{\text{all gridpoints}}$ = 11.20% - 12.02% = -0.82% with a 95% CI of [-0.99, -0.65]
$G1\text{-}G2_{\text{ocean only}}$ - $G1\text{-}G2_{\text{all gridpoints}}$ = 12.57% - 12.02% = 0.54% with a 95% CI of [0.39, 0.69]
<u>DJF High Cloud Differences</u>
$G1\text{-}G2_{\text{land only}}$ - $G1\text{-}G2_{\text{all gridpoints}}$ = 7.24% - 6.38% = 0.86% with a 95% CI of [0.81, 0.91]
$G1\text{-}G2_{\text{ocean only}}$ - $G1\text{-}G2_{\text{all gridpoints}}$ = 5.81% - 6.38% = -0.57% with a 95% CI of [-0.61, -0.53]
<u>JJA Low Cloud Differences</u>
$G1\text{-}G2_{\text{land only}}$ - $G1\text{-}G2_{\text{all gridpoints}}$ = -6.56% - -7.30% = 0.74% with a 95% CI of [0.6, 0.87]
$G1\text{-}G2_{\text{ocean only}}$ - $G1\text{-}G2_{\text{all gridpoints}}$ = -7.78% - -7.30% = -0.49% with a 95% CI of [-0.58, -0.4]
<u>JJA High Cloud Differences</u>
$G1\text{-}G2_{\text{land only}}$ - $G1\text{-}G2_{\text{all gridpoints}}$ = 3.34% - 3.69% = -0.35% with a 95% CI of [-0.4, -0.29]
$G1\text{-}G2_{\text{ocean only}}$ - $G1\text{-}G2_{\text{all gridpoints}}$ = 3.92% - 3.69% = 0.23% with a 95% CI of [0.2, 0.26]

In all months for all cloud types, the group difference G1-G2 between all gridpoints and land gridpoints/all gridpoints and ocean gridpoints is never more than 1% within the 95% confidence interval, which is much less than the average difference between Group 1 and Group 2. For this reason, we think it is appropriate to perform our calculations using all gridpoints. We added a comment about these results to lines 174-176.

**Page 6, L191: shouldn't you do this by season (winter-summer) or at least comment on differences between winter and summer PDFs. Maybe show a sub set?**

We constructed winter (DJF) and summer (JJA) PDFs for the cloud influencing factors:

DJF:

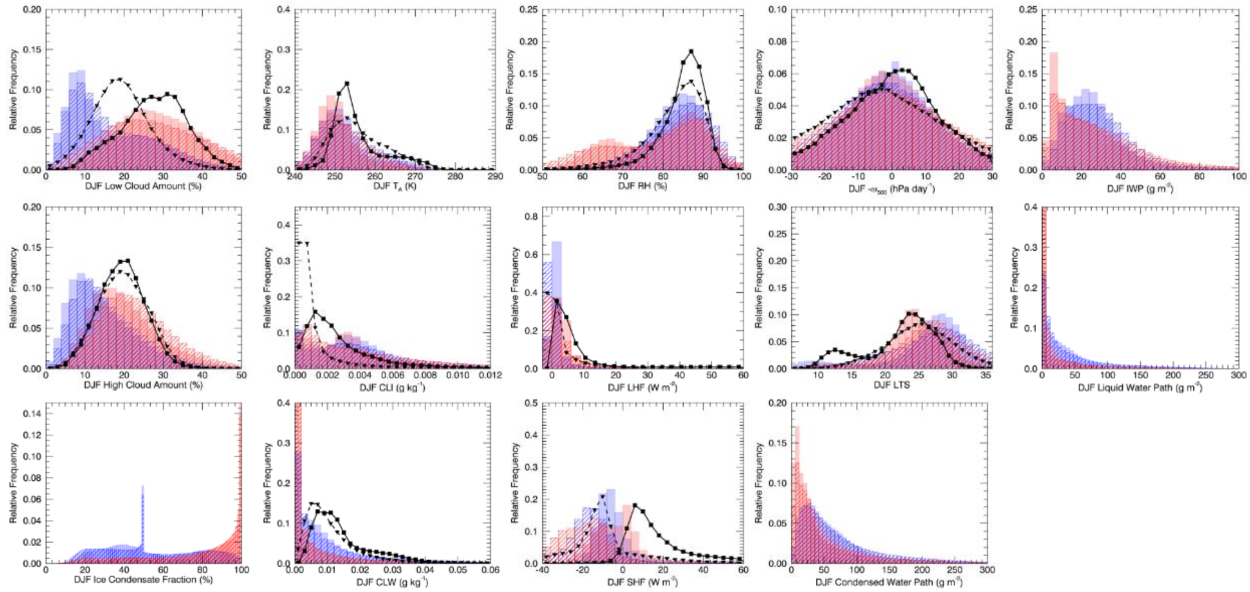


And JJA:

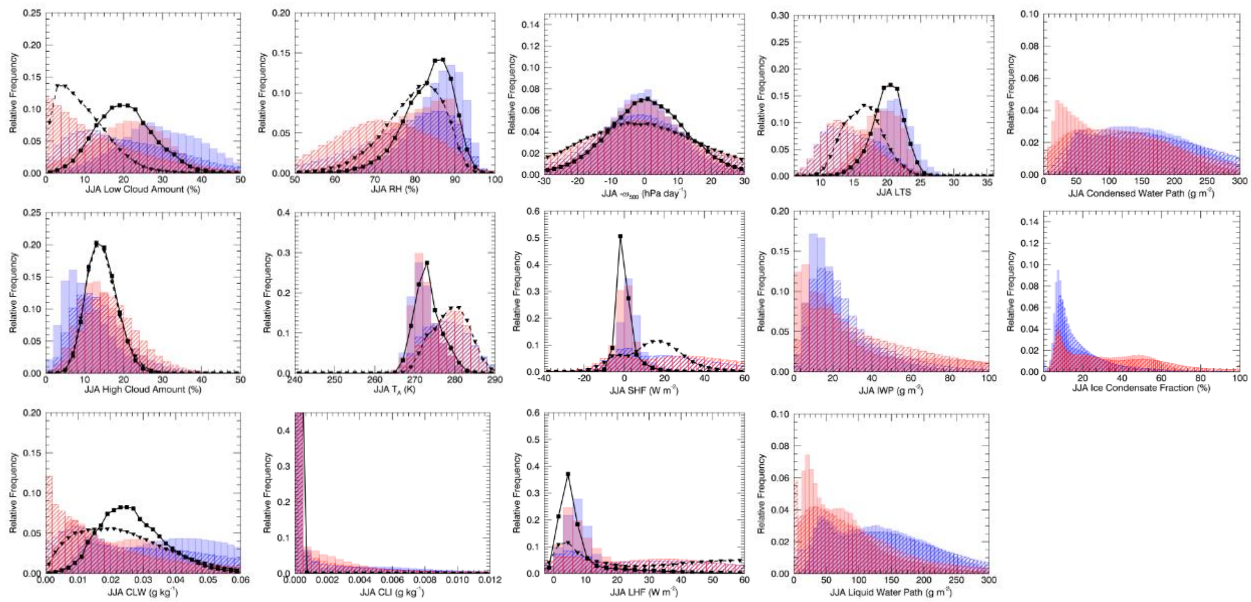


While the average values of these quantities/shape of the PDF differ between DJF, JJA, and all months, the relative characteristics between model groups remains consistent (i.e. Group 1 models are drier, have lower stability, larger ice fraction, and a smaller amount of liquid condensate).

**Page 6, L215: why are there vertical stripes here? Is this one model? Does it represent anything physical?**

The stripes result from two models, bcc-csm1-1 and NorESM1-ME, and do not represent anything physical.

Reviewer Responses for Referee #2

**1) Let us remind ourselves that we are in the Arctic, the region that has been chronically problematic not only for models, but also for observations and reanalysis datasets. I can't help but wonder if the conclusions would change if the authors use ERAInterim/ERA5/JMA etc. instead of MERRA-2. Hinging their conclusions drawn from the stratification analysis (esp LTS, w) only on MERRA 2 is a bit risky.**

We agree with you that reanalysis in the Arctic has significant problems, especially in the lower tropospheric temperature profile. However, we would like to clarify that the results of our analysis do not hinge on a reanalysis. The stratification analysis is performed with CMIP5 model output LTS, vertical velocity, and low cloud amount. In the future observational analysis the reanalysis used must be a prime consideration. To provide an additional reanalysis perspective, we have now included ERA-Interim in the analysis of Arctic cloud amount (e.g. Figs. 1 and 2).

**2) The parameters like LWP and IWP have the largest uncertainties, no matter if you analyse reanalysis or observational data. How does this play a role? Also, can all models explicitly resolve cloud ice and cloud liquid water separately? Or does the partitioning depend on the temperature profile?**

Referee #1 suggested that a table giving more details of the model microphysics schemes would be helpful, and we agree. In Table 1, we have provided a short description of how each model obtains cloud ice and liquid; many models do calculate cloud liquid and ice separately, while others calculate a single mixing ratio of total water, and use a temperature dependent partition to obtain liquid and ice. Both types of models are present in Group 1 and Group 2, indicating that a model's specific microphysics scheme is not solely responsible for the seasonal cycle biases. For example, we may hypothesize that models that obtain cloud ice and liquid individually rather than a total condensate more accurately represent Arctic mixed phase clouds, but if these models also had too coarse a vertical resolution to resolve the supercooled liquid water layer, we would not see an improvement in the simulation of cloud amount. This is not to say that the way in which models treat cloud water phase is not important, only that the complexity of GCMs is such that any one parameterization alone cannot explain the cloud fraction differences we see. We found *Komurcu et al 2014* ("Intercomparisons of the cloud water phase among global climate models") to be an informative resource; they studied the response of simulated cloud phase in GCMs to changes in ice nucleation schemes and found that implementing the same ice nucleation scheme in all of the models did not reduce the spread in cloud phase.
In response to Referee #1, we grouped the models by those that prognostically calculate both ice and liquid, and those that calculate a single mixing ratio of total water and use a temperature dependent partitioning to determine cloud ice and liquid and plotted joint distributions of CA, CLI, CLW, and ice fraction. Please see the discussion on the differences in model parameterizations above in the response to reviewer #1.

**3) Over the Arctic Ocean, what kind of biases in the annual cycles of cloudiness models show if they are stratified according to sea-ice conditions, for example, permanently sea-ice covered regions versus completely ice-free regions?**

We have plotted seasonal cycles of cloud fraction for three surface types to address this comment: (Land: top left; Ocean: top right; Sea ice: bottom left)

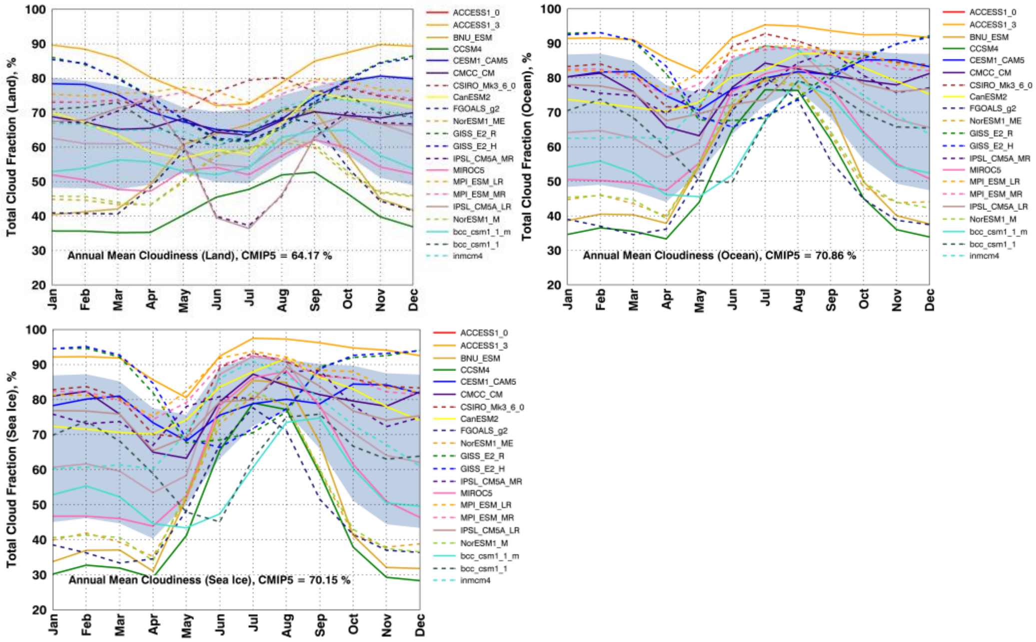


The similarities in seasonal cycle biases between the three surface types include 1) the largest model spread occurring in winter, and 2) the same models with too few winter clouds over the entire domain also have too few winter clouds over each surface type (and vice versa for those models with too many winter clouds). The largest difference between the three surface types is found during summer, where land shows a smaller cloud fraction than either ocean or sea ice. Additionally, even though the general shape of each models' seasonal cycle is similar across surface types, the seasonal amplitudes (winter versus summer) are greatest over sea ice and ocean and damped over land.

**4) The differences in the representation of dynamical meteorology among models are also importing while interpreting the results. For example, do models show similar heat and moisture transport into the Arctic, which has a strong influence on cloudiness?**

This is a very interesting and important question. Previous work (e.g., Morrison et al. 2012) highlights the important role that moisture advection plays in the maintaining low-level mixed phase clouds in the Arctic. Moreover, Boisvert et al. (2016) show the important effect that moisture transport by storms can have on Arctic sea ice and clouds. However, moisture advection/transport is a metric and process that we think is inadequately represented and potentially misrepresented by monthly averaged data. Therefore, we have decided to not include analysis of the influence of dynamics here. We recommend and will incorporate this comment into our future work, as we agree with you that atmospheric dynamics and moisture transport is a key consideration here. Addressing the role of dynamics requires the use of daily model output.

**References**

Boisvert, L.N.; Petty, A.A.; Stroeve, J.C. The Impact of the Extreme Winter 2015/16 Arctic Cyclone on the Barents–Kara Seas. Mon. Weather Rev. 2016, 144, 4279–4287.

Komurcu, M., Storelvmo, T., Tan, I., Lohmann, U., Yun, Y., Penner, J. E., Wang, Y., Liu, X., and Takemura, T. (2014), Intercomparison of the cloud water phase among global climate models, *J. Geophys. Res. Atmos.*, 119, 3372– 3400, doi:10.1002/2013JD021119.

Kretzschmar, J., Salzmann, M., Mülmenstädt, J., and Quaas, J.: Arctic cloud cover bias in ECHAM6 and its sensitivity to cloud microphysics and surface fluxes, Atmos. Chem. Phys. Discuss., https://doi.org/10.5194/acp-2018-1135, in review, 2018.

Morrison, H.; de Boer, G.; Feingold, G.; Harrington, J.; Shupe, M.D.; Sulia, K. Resilience of persistent Arctic mixed-phase clouds. Nat. Geosci. 2012, 5, 11–17.

# On Arctic cloud annual cycle biases in climate models

Patrick C. Taylor*

NASA Langley Research Center, Climate Science Branch, Hampton, Virginia

Robyn C. Boeke

Science Systems Applications Inc., Hampton, Virginia

Ying Li and David W.J. Thompson

Colorado State University, Department of Atmospheric Science, Fort Collins, Colorado

*Corresponding author address: Patrick C. Taylor, NASA Langley Research Center, 21 Langley Blvd. MS:420, Hampton, VA, 23681 (patrick.c.taylor@nasa.gov)

Formatted: Left

## Abstract

Arctic clouds exhibit a robust annual cycle with maximum cloudiness in fall and minimum in winter. These variations affect energy flows in the Arctic with a large influence on the surface radiative fluxes. Contemporary climate models struggle to reproduce the observed Arctic cloud amount annual cycle and significantly disagree with each other. The goal of this analysis is to quantify the cloud influencing factors that contribute to winter-summer cloud amount differences, as these seasons are primarily responsible for the model discrepancies with observations. We find that differences in the total cloud amount annual cycle are primarily caused by differences in low, not high, clouds; the largest differences occur between the surface and 950 hPa. Grouping models based on their seasonal cycles of cloud amount and stratifying cloud amount by cloud influencing factors, we find that model groups disagree most under strong lower tropospheric stability, weak to moderate mid-tropospheric subsidence, and cold lower tropospheric air temperatures. Inter-group differences in low cloud amount are found to be a function of the dependence of low cloud amount on the lower tropospheric thermodynamic characteristics. We find that models with a larger low cloud amount in winter maintain a larger fraction of cloud ice, whereas models with a larger low cloud amount in summer have a larger fraction of cloud liquid. Thus, the parameterization of ice microphysics and cloud liquid and ice partitioning, contributes to the inter-model differences in the Arctic cloud annual cycle and provides further evidence of the important role that cloud ice microphysical processes play in the evolution and modeling of the Arctic climate system.


**Deleted:** S

**Deleted:** produce more

**Deleted:** produce more

**Deleted:**

**Formatted:** Not Highlight

**Deleted:** , specifically the ice formation mechanism (deposition vs. immersion freezing)

## 1. Introduction

Arctic clouds, arguably one of the most poorly understood aspects of the Arctic climate system, strongly modulate radiative energy fluxes at the surface, through the atmosphere, and to the top of the atmosphere (Curry et al. 1996; Shupe and Intrieri 2004; Kay et al. 2008; Cesana et al. 2012; Kay and L'Ecuyer 2013). As such, Arctic clouds have the potential to influence climate variability and change in the Arctic and globally. For instance, the presence of clouds in winter over sea ice can be the difference between a -40 W $m^{-2}$ surface radiative energy imbalance and a balanced surface radiation budget, influencing surface temperature and sea ice growth rate (Persson et al. 2002; Morrison et al. 2012; Persson et al. 2016). Accurately representing clouds in climate models is therefore necessary to realistically simulate the evolution of the Arctic surface energy budget.

Contemporary climate models, however, strongly disagree with observations on the seasonality of Arctic cloud radiative effects. Observations indicate that Arctic clouds cool the surface through the reflection of solar radiation for a few months during summer and warm the surface through enhanced downwelling longwave radiation the rest of the year (Shupe and Intrieri 2004; Kay and L'Ecuyer 2013). Climate models possess significant biases in the seasonality of the surface cloud radiative effect (Karlsson and Svensson 2011; Karlsson and Svensson 2013; Boeke and Taylor 2016). Climate models participating in the Coupled Model Intercomparison Project 5 (CMIP5; Taylor et al. 2012) simulate Arctic clouds that are too reflective in summer and not insulating enough in winter. These cloud radiative effect biases trace to a number of errors in cloud properties: namely, insufficient Arctic cloud amount (English et al. 2015), inaccurate partitioning of cloud water between the liquid and ice phase leading to excessive ice clouds (Li et al. 2012; Cesana et al. 2012; Kay et al. 2016) and insufficient supercooled liquid clouds (Komurcu et al. 2014). This study focuses on errors in model-simulated Arctic cloud amount and its annual cycle.

Arctic cloud amount exhibits a robust annual cycle that has been known for some time (e.g., Huschke 1969; Hahn et al. 1995). However, important revisions to our understanding of the cloud amount annual cycle have occurred since the launch of the CloudSat Cloud Profiling Radar (Stephens et al. 2008) and the Cloud-Aerosol Lidar with Orthogonal Polarization (CALIOP; Winker et al. 2007). As illustrated in Liu et al. (2012), both ground observer and satellite passive radiometer retrieval data sets indicate a broad summer maximum in cloud amount extending into September, declining through fall, and reaching an annual cycle minimum in winter. Both data sets suffer from the lack of sunlight in fall and winter. Passive cloud retrieval algorithms also change with surface type, posing additional challenges (e.g., Minnis et al. 2011a,b). CALIOP and CloudSAT active remote sensing instruments provide cloud amount data independent of surface type with high accuracy in the absence of sunlight. Active remote sensing observations indicate that average Arctic cloud amount exceeds 65% for each month reaching ~90% in fall (Liu et al. 2012; Boeke and Taylor 2016) and that previous data sets missed ~10-15% of fall cloud cover. Space-based active retrievals are not without limitations, most important of which is a 25-40% under-detection of clouds below 500 meters relative to surface-based remote sensing observations (Liu et al. 2017). However, CALIOP and CloudSAT cloud amount data still provide the most complete characterization of vertically-resolved Arctic-wide cloud amount.

**Deleted:**

Despite the refined observational knowledge of the Arctic cloud annual cycle, the mechanisms that control it remain an open question. Beesley and Moritz (1999) outline several physical controls on Arctic clouds including surface-atmosphere coupling, large-scale meteorology, and cloud microphysics. The surface-atmospheric coupling mechanism implies—less sea ice, more surface evaporation—that Arctic cloud amount should follow the annual cycle of sea ice. Observationally, this mechanism has been shown to operate under specific conditions in fall, whereby reduced sea ice cover corresponds to increased cloud amount, but not in summer (Kay and Gettelman 2009; Taylor et al. 2015; Morrison et al. 2018). Second, seasonal changes in large-scale meteorology, atmospheric advection, and humidity influence the cloud amount annual cycle. Previous work demonstrates a significant dependence of cloud properties on local atmospheric conditions (Kay and Gettelman 2009; Barton et al. 2012; Li et al. 2014; Liu and Schweiger 2017). Lower tropospheric stability has a profound influence on Arctic low cloud amount, whereby increased stability corresponds to reduced cloud amount (Taylor et al. 2015). Third, cloud microphysical processes affect cloud amount and exhibit a seasonality tied to temperature, whereby colder temperatures support ice crystal formation (e.g. via the Wegener-Bergeron-Findeisen process or heterogeneous freezing) (Beesley and Moritz 1999). The growth of ice crystals consumes available liquid, leading to precipitation. Once all of the ice has fallen out, the atmosphere transitions from cloudy to clear (Pithan et al. 2014). In addition, the seasonality of aerosol amount and composition can influence cloud amount and properties by altering microphysics (e.g., Jackson et al. 2012; Coopman et al. 2018).

**Deleted:** and precipitation

**Deleted:**

**Formatted:** Highlight

Given the lack of mechanistic understanding of the drivers of the Arctic cloud annual cycle, it comes as no surprise that climate models struggle to simulate the Arctic cloud amount annual cycle. Comparison of the CALIOP-CloudSAT total column cloud amount with CMIP5 models indicates that individual models differ from observations by more than 15% in summer and 40% in winter (Boeke and Taylor 2016). Further, Boeke and Taylor (2016) show that several models produce peak cloud cover in winter with others producing peak cloud cover in summer; few models capture the observed fall cloud cover peak. Thus, the majority of models misrepresent the annual cycle of Arctic cloud cover. Meteorological reanalysis data products are not immune and also exhibit similar errors in the Arctic cloud amount annual cycle timing (Liu and Key 2016).

The combination of poor model simulation and the lack of mechanistic understanding of the drivers of the Arctic cloud annual cycle signals a critical gap in our understanding with significant consequences for our ability to attribute, simulate, and predict Arctic climate variability and change. We address this gap by investigating the drivers of the inter-model differences in the Arctic cloud annual cycle in CMIP5 climate models. As previous studies indicate, Arctic cloud amount is influenced by its environment; a fact that guides this analysis. We adopt a methodology stratifying climate model simulated vertically-resolved cloud amount by several key cloud influencing factors, described in Section 2. The stratification methodology, discussed in Section 3, enables us to explore the dependence of simulated cloud amount on individual and groups of cloud influencing factors and how they differ across the CMIP5 models. In section 4, our key results are compared with previous work (e.g, Li et al. 2014) and our understanding of the mechanisms driving the Arctic cloud annual cycle is discussed. Lastly, Section 5 highlights the insights gained into how the Arctic cloud annual cycle influences Arctic climate variability and change and our ability to reproduce it.

## 2. Methodology and Models

The goal of this analysis is to explain the divergent representations of the Arctic cloud amount annual cycle found in contemporary climate models. We use the historical forcing simulations (prescribed greenhouse gases and land use changes consistent with observations from 1979-2005) from 24 CMIP5 climate models (Taylor et al. 2012) with the available output in the archive (https://esgf-node.llnl.gov/projects/cmip5/). Monthly mean variables used include vertically-resolved cloud amount, air temperature ($T_A$), relative humidity (*RH*), 500 hPa vertical velocity ($\omega_{500}$), sensible heat flux (*SHF*), latent heat flux (*LHF*), liquid and ice water mixing ratios (*CLW* and *CLI*, respectively), ice water path and total water path (*IWP* and *CLWVI*, respectively), sea ice concentration (*SIC*) and lower tropospheric stability (*LTS*). Lower tropospheric stability is defined as the potential temperature difference between the surface and 700 hPa, computed from the monthly-averaged temperature profile. Table 1 lists each CMIP5 model, institution, a model cloud and microphysics scheme description, and relevant references.

Several observed and reanalysis variables are included as a reference to gauge the fidelity of the model results. The Modern-Era Retrospective Analysis for Research and Applications-2 (MERRA-2) provides information on the Arctic atmospheric conditions and their covariances. MERRA-2 has a horizontal resolution of 0.5° latitude x 0.625° longitude and vertical resolution of 72 hybrid-eta levels fully described in Bosilovich et al. (2015) and Molod et al. (2015). The observed vertically-resolved Arctic cloud amount are derived from CALIPSO-CloudSAT-CERES-MODIS (C3M) data (Kato et al., 2010). Vertical profiles of cloud fraction are also included from ERA-Interim reanalysis (Dee et al. 2011).

The primary methodology composites cloud amount into bins of individual cloud influencing factors, adapted from Li et al. (2014). The cloud influencing factors considered include $\omega_{500}$, *LTS*, *SHF*, *LHF*, *SIC*, *IWP*, *CLWVI*, and vertically-resolved $T_A$ and *RH*. The primary difference between the present analysis and Li et al. (2014) is the use of monthly-averaged model output instead of instantaneous satellite data. We also extend our composite analysis beyond single variables and construct joint distributions. To understand the potential shortcomings of using monthly-averaged output instead of daily output calculations were also carried out using daily data obtained from the one available model (IPSL-CM5A-LR). The results indicated that the largest difference using daily in place of monthly mean model output was the limited dynamic range at monthly scales. The daily and monthly mean results agree in the most frequently occurring meteorological conditions. Thus, the use of monthly averaged data does not affect the main conclusions.

**Deleted:** s

**Deleted:** In order t

**Formatted:** Not Highlight

**Deleted:** validate the

**Deleted:** of

**Formatted:** Not Highlight

**Formatted:** Not Highlight

**Deleted:** e

**Formatted:** Not Highlight

**Deleted:** ,

**Formatted:** Not Highlight

**Deleted:** presented in this paper were

**Formatted:** Not Highlight

**Formatted:** Not Highlight

**Formatted:** Not Highlight

**Formatted:** Font: Times

**Formatted:** Not Highlight

**Deleted:** ; applying our

**Formatted:** Not Highlight

**Deleted:** methodology to daily data reproduced low cloud amount with the same accuracy as monthly results

**Formatted:** Highlight

Lastly, the results are composited and analyzed within two groups based upon key features of the simulated Arctic total cloud amount annual cycle. Figure 1a shows that the cloud amount annual cycles from individual models tend to follow one of two patterns: one showing the largest cloud amount in winter and small seasonal variations, and another showing minimum cloud amount in winter, peak summertime/early autumn cloud amount, and large seasonal amplitude. Figure 2 summarizes these two patterns showing a scatterplot of the average winter (DJF) and summer (JJA) cloud amounts for individual models motivating the separation of the 24 models into two groups; models that simulate a larger total cloud amount in winter are referred to as Group 1 (10 models), whereas models that simulate a larger total cloud amount in summer are referred to as Group 2 (14 models). C3M observations and ERA-Interim and MERRA-2 reanalysis are denoted with star symbols. While the models can be grouped in several different ways, the choice to delineate model groups above and below the diagonal 1:1 line in Fig. 2 clearly places models with similar cloud amount annual cycle shapes together while also grouping them based on how they differ from observations. Group 1 models most closely resemble MERRA-2 and show maximum cloud amount in winter, differing from C3M observations that show minimum cloud amount in winter. Group 2 models correctly simulate the season of minimum cloud amount from C3M (winter), but possess a much larger-amplitude annual cycle than either C3M or reanalysis and a summer peak in cloud amount as opposed to fall, as seen in both C3M and ERA-Interim. This separation is also motivated by the need to understand the factors (e.g., microphysics, surface turbulent fluxes, dynamics, and thermodynamics) responsible for producing clouds in these individual seasons and to provide insight as to the cause(s) of Arctic cloud amount annual cycle differences between models. The application of this grouping allows us to consolidate the analysis and take a deeper look at the influencing factors.

**Deleted:** fail to reproduce the correct timing of the maximum cloud amount, showing peak cloud amount in winter while C3M shows

## 3. Results

### a. Vertical variations of the cloud amount annual cycle

Figure 3 illustrates the vertically-resolved average cloud amount annual cycle for each group. Group 1 (Fig. 3a) exhibits a minimum in low cloud amount (>850 hPa) in May through July with maximum low cloud amount in January and February. Group 1 high cloud amount follows a similar seasonal pattern as low clouds with a minimum in summer and maximum in the fall/winter at reduced amplitude. Group 2 (Fig. 3b) exhibits a similar high cloud amount annual cycle as Group 1 with smaller cloud amounts and a weaker amplitude. However, the annual cycle of low cloud indicates that cloud amount slowly increases in amount and extends in height through summer, then sharply decreases after September, in sharp contrast with C3M observations and MERRA-2 reanalysis (Fig. 3f,g) and Group 1. ERA-Interim (Fig. 3h) shows a similar increase in low cloud amount and vertical extent in late summer peaking in late autumn. Observations and reanalysis (Fig. 3g-h) and Group 1 all agree on the timing of minimum cloud amount during summer. The standard deviation in cloud amount across each group (Fig. 3d,e) indicates that the largest intra-group differences occur at vertical levels and times of year with the largest cloud amount, below 800 hPa and above 500 hPa in winter for both groups and below 800 hPa in summer. The only exception is in Group 1 where larger standard deviations occur in summer below 800 hPa, when Group 1 models show minimum cloud amount. For both groups, the standard deviation in cloud amount is greatest in the lowest levels of the atmosphere during all months.

Figure 1b,c illustrates the model seasonal cycles of Arctic cloud amount for low clouds (1000-850 hPa) and high clouds (500-300 hPa), respectively, as well as for C3M, MERRA-2, and ERA-Interim. The results in Figs. 1b,c demonstrate that low clouds predominantly contribute to the winter versus summer peaks in the simulated seasonal cycle of the total cloud amount. The rest of

**Deleted:** throughout

**Deleted:**

**Deleted:** the

**Deleted:** , but

**Deleted:** s

**Deleted:**

**Deleted:** inter-

**Deleted:** difference in the

this paper analyzes how the dependence of cloud amount on the cloud influencing factors contributes to these differences in Arctic low cloud amount in winter versus summer. The goal of this paper is to understand how, why and to what extent do the cloud influencing factors contribute to the differences in the Arctic low cloud amount with winter peaks in Group 1 and late summer peaks in Group 2.

b. Horizontal variation in the cloud amount annual cycle

The above differences in the annual cycle of the Arctic clouds between Groups 1 and 2 are based on the averages over the entire Arctic region, in this subsection, we further confirm that such differences are spatially uniform. Figure 4 illustrates the spatial variations of the low and high cloud amount differences for Group 1 minus Group 2. In winter, Group 1 produces an average of 12% more low clouds than Group 2 (Fig. 4a) and 7.3% fewer low clouds in summer (Fig. 4c). These differences are generally spatially uniform. Differences in high cloud amount show similar spatial uniformity but with Group 1 producing more high clouds than Group 2 in both winter (+6.4%) and summer (+3.7%) (Fig. 4b,c). These differences show weak spatial variability. Comparing the differences in the average cloud amount of land, ocean, and all surface types indicates that the differences are generally less than 1% for high and low cloud amount; and, indicate that regional differences do not significantly contribute to the annual cycle differences in low or high cloud amount.

Since atmospheric and surface properties vary across the Arctic and can influence the simulated cloud amount, we also analyze the spatial variations in the cloud influencing factors for the model groups (not shown) finding that the differences between Group 1 and 2 exhibit a general spatial uniformity with minor deviations. As such, the following stratification analysis is performed over the entire Arctic region.

Deleted: s

Deleted: .4

Deleted:

Formatted: Font: Times

Deleted: These differences show weak spatial variability

Deleted: and thus

c. Inter-group differences in mean and distribution of atmospheric conditions

Arctic cloud formation is influenced by a number of atmospheric characteristics including surface and boundary layer thermodynamic properties and large-scale dynamics (e.g., Kay and Gettelman 2009). Table 2 and Figure 5 provide the annual-mean ensemble averages of cloud influencing factors for each group and their probability density function (PDF) over the ocean and land surfaces. The average properties in Table 2 for the two groups are generally similar. A difference of means tests between the groups show statistically significant differences for all cloud influencing factors at 95% confidence. Intergroup differences for most cloud influencing factors, however, are small suggesting that differences in average atmospheric conditions do not drive intergroup differences in the cloud amount annual cycle. Notable exceptions are *LTS*, *RH* and *CLW* over both surface types. Group 2 possesses higher *RH* values and almost twice the average *CLW* of Group 1 as well as higher stability. Overall, the spread in the average cloud influencing factors is larger within each group than between Group 1 and 2.

The variability of individual cloud influencing factors is consistent between the groups with some small differences. The PDFs in Fig. 5 summarize the frequency of the cloud influencing factors for Group 1 (red) and Group 2 (blue) separated into land (cross-hatching) and ocean (solid). Figure 5 includes PDFs of each variable derived from MERRA-2 reanalysis and shown in solid black lines for ocean (square symbols) and land (triangle symbols). In most cases, the distribution of cloud influencing factors is similar between the two groups for each surface type. The most notable differences between the groups are (1) Group 2 models exhibit a higher frequency of stronger *LTS* values for both land and ocean (Fig. 5a) and (2) Group 2 $-\omega_{500}$ exhibits a higher frequency of values near 0 hPa day$^{-1}$ over both land and ocean (Fig. 5b). In these cases, Group 1 $-\omega_{500}$ and *LTS* is more consistent with MERRA-2. Additional group differences are seen in *RH* (Fig. 5g),

Deleted: 1

Deleted: 1

Formatted: Font: Italic

Formatted: Font: Italic

**Commented [MOU1]:** Robyn: we need to verify that this is correct.

**Commented [RB2]:** Std devs for each group calculated and this is correct

Formatted: Font: Italic

Formatted: Font: Italic

Formatted: Font: Italic

Formatted: Font: Italic

Formatted: Font: Italic

Formatted: Font: Italic

Deleted: over land and ocean and

Deleted: over ocean

*CLI* (Fig. 5d) and *CLW* (Fig. 5h) whereby Group 2 favors higher *RH*, larger *CLW*, and a higher frequency of *CLI* values near 0 g kg$^{-1}$ while Group 1 shows a higher frequency of *CLW* values near 0 g kg$^{-1}$.

d. Dependence of vertically-resolved cloud amount on cloud influencing factors

We investigate the possibility that intergroup differences in cloud amount are explained by differences in the relationship between cloud amount and cloud influencing factors. Figure 6 shows the vertically-resolved average cloud amount binned by five different cloud influencing factors ($-\omega_{500}$, *LTS*, ice water path (*IWP*), total condensed water path (*CLWVI*; ice plus liquid), and *SIC*. Since Group 1 models show a winter cloud amount peak in the annual cycle, it is expected that Group 1 produces larger cloud amounts than Group 2 throughout the troposphere and especially below 850 hPa for most cloud influencing factors (Fig. 6, right column). Figure 6a,b illustrates the cloud vertical structure as a function of $-\omega_{500}$ and reveals a general increase in cloud amount as the strength of rising motion increases at most levels for both groups over ocean (from left to right in Fig. 6a,b) and land (Fig. S1). Group 1 exhibits a deviation from this behavior at pressures >950 hPa showing almost no dependence on $-\omega_{500}$; cloud amount is large under both sinking and rising motion. The inter-group differences (Fig. 6c) indicate that Group 1 produces larger cloud amount than Group 2 throughout the troposphere and particularly at pressures >950 hPa.

Figure 6d,e illustrates a similar dependence of the vertically-resolved average cloud amount stratified by *LTS*. Both groups exhibit a general decrease in cloud amount with stronger *LTS* at all levels and over both ocean and land (Fig. S1); in other words, as conditions become more stable clouds tend to occur in a shallower layer closer to the surface. Much like $-\omega_{500}$, Group 1 produces equal or larger cloud amounts at pressures >950 hPa as *LTS* increases, signaling a potentially important $-\omega_{500}$-*LTS* covariance (discussed below). Specifically, the average cloud amount is >20%

**Deleted:** and

**Deleted:** a larger *CLI* and

**Deleted:** )

**Formatted:** Font: Italic

**Deleted:** d

**Formatted:** Font: Italic

**Formatted:** Font: Italic

**Formatted:** Font: Italic

larger in Group 1 than in Group 2 when *LTS* > 20 K at pressures >950 hPa. The larger cloud amounts at pressures >950 hPa can be viewed as either a difference in a dissipative mechanism (e.g., turbulent mixing, cloud microphysics, or precipitation) between the groups or a difference in cloud production (e.g., ice formation or surface buoyancy).

Figure 6g,h,j,k illustrates the dependence of cloud amount on *IWP* and *CLWVI*. Models in both groups favor more cloud amount with higher cloud bases for increasing *IWP* and *CLWVI*; both surface types exhibit similar behavior. Group 1 diverges from Group 2 at lower values of *IWP* and *CLWVI* (< ~35 g $m^{-2}$) by producing maximum cloud amount in the thin cloud regime at pressures >950 hPa (Fig. 6g,j) while Group 2 shows minimum cloud amount. For the average wintertime values of *IWP* (~32 g $m^{-2}$) and *CLWVI* (~52 g $m^{-2}$), Group 1 has larger cloud amount than Group 2 at all levels over ocean and land.

The influence of surface conditions on cloud amount over the Arctic Ocean is assessed using *SIC*. Representing an integral measure of the surface influence on cloud amount, increased *SIC* generally corresponds to decreases in surface turbulent fluxes and stronger *LTS* (Pavelsky et al. 2011; Taylor et al. 2018). Figure 6m,n illustrates that both groups produce a decrease in cloud amount and lower cloud bases with increased *SIC*; the cloud amount decrease is muted in Group 1 compared to Group 2 (Fig. 6o) as with *LTS*. However, the inter-group differences at high *SIC* values are smaller than for *LTS* (Fig. 6f,o). Overall, the inter-group differences illustrate a weak dependence on *SIC* in winter.

Figure 7 shows the vertically-resolved average cloud amount dependence on four different cloud influencing factors ($-\omega_{500}$, *LTS*, *IWP*, and *CLWVI*) over land and one (*SIC*) over ocean for summer (JJA). Since Group 2 includes models with a summer cloud amount peak in the seasonal cycle (especially for low clouds), it is expected that Group 2 models generally produce larger cloud

**Formatted:** Font: Italic

**Formatted:** Font: Italic

**Deleted:** five

**Deleted:** , and *SIC*

**Deleted:** (excluding

**Deleted:** , which is

**Deleted:** )

amount than Group 1 throughout the troposphere for almost all cloud influencing factors (right column). We show results over land in summer because differences exceed 20% over land and are 5-10% over ocean. The largest inter-group differences are again at pressures >950 hPa, in this case exhibited by Group 2 rather than Group 1. Important findings from Fig. 7 include (1) the inter-group differences in cloud amount are ~5-10% smaller during summer, (2) Group 2 tends to produce more clouds at pressures >950 hPa for all cloud influencing factors, (3) all dependencies of cloud amount on cloud influencing factors are weaker than in winter, and (4) neither group exhibits a dependence of the average cloud fraction on *SIC*. Only cloud amount dependencies with $-\omega_{500}$, *IWP*, and *CLWVI* illustrate a noteworthy gradient in summer where Group 2 produces a stronger low cloud amount increase as rising motion increases and at larger *IWP*/*CLWVI* values.

The winter and summer analyses reveal several key takeaways. First, the primary intergroup differences are found at pressures >950 hPa in the thin low cloud regime (IWP< 30 g m$^{-2}$) in winter and the thicker low cloud regime (IWP > 70 g m$^{-2}$) in summer. Second, the differences in the cloud amount dependence on cloud influencing factors are larger during winter than summer. Third, the largest inter-group differences in winter are found under stable conditions and sinking motion and in summer under rising motion. The fact that intergroup differences in the cloud amount dependence are largest for *LTS* and $-\omega_{500}$ and the expectation of significant covariances between these two variables warrants simultaneous analysis using a joint distribution to address the question, why are Group 1 models able to maintain large low cloud fraction under strong stability and subsidence?

e. Joint PDFs: *LTS* and $-\omega_{500}$

Figure 8 shows the joint distribution of average low cloud amount stratified by both *LTS* and $-\omega_{500}$ (Fig. 8a-b) with the corresponding frequency of occurrence of each bin in winter

**Deleted:** and
**Deleted:** as
**Deleted:** increase
**Deleted:** s
**Deleted:**
**Formatted:** Superscript
**Deleted:** .
**Deleted:** ly
**Deleted:** c
**Deleted:** and

contoured over top for Group 1 (Fig. 8a) and Group 2 (Fig. 8b). Cloud amount depends on (1) the relationship between the cloud amount and *LTS* and $-\omega_{500}$ and (2) how frequently each LTS and $-\omega_{500}$ bin occurs. For regions with *LTS* < 12 K, low cloud amount for both groups is primarily a function of *LTS* with little dependence on $-\omega_{500}$; the intergroup differences illustrate the same behavior (Fig. 8c). Considering *LTS* >12 K, low cloud amount exhibits a dependence on both *LTS* and $-\omega_{500}$, however the intergroup differences (Fig. 8c) still correspond with only to variations in *LTS*.

While both groups simulated the highest frequency of occurrence of $-\omega_{500}$ bin around -4 hPa day$^{-1}$, Group 1 most frequently simulates LTS values between 22-24 K whereas Group 2 simulates slightly higher values between 26-30 K (Fig. 8a,b contours). Thus, the inter-group difference is marked by a dipole pattern along the LTS axis between 22-24 K and 26-30 K, and these regions contribute most to the winter low cloud amount between Group 1 and Group 2.

Figure 9 shows the joint distribution of low cloud amount by *LTS* and $-\omega_{500}$ bins and the corresponding frequency of occurrence in summer. The pattern in the summer average low cloud amount illustrated in Fig. 9a,b is more similar between the groups than in winter yielding smaller inter-group differences (Fig. 9c). First considering *LTS*<14 K, low cloud amount depends primarily on *LTS* with a weak dependence on $-\omega_{500}$. Next considering *LTS*>14 K, low cloud amount depends on both *LTS* and $-\omega_{500}$, a behavior similar to winter. Additionally, the low cloud amount gradients are sharper in summer than winter, meaning that summer low cloud amount is more susceptible to small changes in *LTS* and $-\omega_{500}$ than in winter. The inter-group differences in frequency of occurrence indicates that Group 2 exhibits higher *LTS* values (20-25 K) and lower *LTS* values (<12 K) more frequently.

The winter or summer average low cloud amount can be estimated from the terms illustrated in Figs. 8 and 9 using

**Deleted:** (Fig. 8d-f)

**Deleted:**

**Formatted:** Font: Italic

**Deleted:**

**Deleted:** d,e

**Deleted:** primarily

$$\overline{LCA} = \sum_{i,j} LCA\left(LTS_i, -\omega_{500,j}\right) * RFO\left(LTS_i, -\omega_{500,j}\right). \qquad (1)$$

This expression describes the weighted sum of the low cloud amount over all $LTS_i$ and $-\omega_{500,j}$ from each $i, j$ bin, where $LCA\left(LTS_i, -\omega_{500,j}\right)$ corresponds to the low cloud amount as a function of $LTS_i$ and $-\omega_{500,j}$ and $RFO\left(LTS_i, -\omega_{500,j}\right)$ corresponds to the relative frequency of occurrence of each $LTS_i$ and $-\omega_{500,j}$ bin. Applying (1) to compute the average low cloud amount, $\overline{LCA}$, in either winter or summer reproduces the winter and summer average low cloud amount for each group to within 1-2% percent (Table 3). We construct $LCA\left(LTS_i, -\omega_{500,j}\right)$ by averaging, thus removing some variability. As such, eq. (1) parameterizes low cloud amount and is not expected to exactly reproduce $\overline{LCA}$. This exercise indicates that $\overline{LCA}$ can be accurately reconstructed using the $LCA\left(LTS_i, -\omega_{500,j}\right)$ and $RFO\left(LTS_i, -\omega_{500,j}\right)$ suggesting that this approach is applicable in interpreting drivers of interannual variability or feedbacks in low cloud amount.

Equation (1) can be applied to both Group 1 and Group 2, and then the inter-group differences (Group 1 minus Group 2; $\overline{\delta LCA_{G1-G2}}$) can be estimated and decomposed using a first-order Taylor series approximation to further quantify the relative contributions from differences in 1) $\delta LCA\left(LTS_i, -\omega_{500,j}\right)$ and 2) $\delta RFO\left(LTS_i, -\omega_{500,j}\right)$.

$$\overline{\delta LCA_{G1-G2}} = \sum_{i,j} \left[\left(\delta LCA\left(LTS_i, -\omega_{500,j}\right)_{G1-G2} * RFO\left(LTS_i, -\omega_{500,j}\right)_{G1}\right)\right] +$$

$$\sum_{i,j} \left[\left(LCA\left(LTS_i, -\omega_{500,j}\right)_{G1} * \delta RFO\left(LTS_i, -\omega_{500,j}\right)_{G1-G2}\right)\right] \qquad (2)$$

In (2), $\overline{\delta LCA_{G1-G2}}$ corresponds to the inter-group difference (Group 1 minus Group 2) in average low cloud amount, $\delta LCA\left(LTS_i, -\omega_{500,j}\right)_{G1-G2}$ corresponds to the inter-group difference in the dependence of low cloud amount on $LTS$ and $-\omega_{500}$ dependence, and $\delta RFO\left(LTS_i, -\omega_{500,j}\right)_{G1-G2}$ corresponds to the inter-group difference in the relative frequency of occurrence of $LTS$ and $-\omega_{500}$

**Formatted:** Font: Italic

**Formatted:** Font: Italic

**Formatted:** Font: Italic

**Formatted:** Font: Italic

**Formatted:** Font: Italic

**Formatted:** Font: Italic

**Deleted:** 2

bins. In this framework, the first term on the right-hand side, $\delta LCA(LTS_i, -\omega_{500,j})_{G1-G2}$, represents the influence of the parameterized cloud physics and the second term, $\delta RFO(LTS_i, -\omega_{500,j})_{G1-G2}$, represents the influence of atmospheric state occurrence. Table 4 summarizes the results and overwhelmingly indicates that the $\delta LCA(LTS_i, -\omega_{500,j})_{G1-G2}$ term is responsible for the summer and winter inter-group differences in low cloud amount.

**Deleted:** 3

While this result attributes the Group 1 minus Group 2 differences to parameterized cloud physics and not the atmospheric state occurrence, it does not explain the fundamental cause. The cause(s) is due to differences in the specifics of the parameterized cloud physics, systematic differences in the atmospheric conditions grouped by *LTS* and -$\omega_{500}$ bins, or a combination of both. A systematic exploration of the intergroup differences in cloud physics parameterizations are beyond the scope of this study. We explore the intergroup differences in atmospheric conditions within *LTS* and -$\omega_{500}$ bins to assess the influence on low cloud amount differences.

Characterizing atmospheric state by *LTS* and -$\omega_{500}$ bins does not account for all intergroup differences in atmospheric state. Thus, we consider atmospheric and surface conditions stratified by *LTS* and -$\omega_{500}$ (Fig. 10). Both groups exhibit similar distributions of lower tropospheric *RH*, 950-hPa $T_A$, *SHF*, *LHF*, and *SIC* (not shown) within the *LTS* and -$\omega_{500}$ bins in winter (Fig. 10) and summer (Fig. S3). Intergroup differences in *RH* (Fig. 10c) are generally <5% and anti-correlate with intergroup low cloud amount differences; in other words, Group 2 exhibits smaller low cloud amount than Group 1 and yet has a larger *RH* and more frequently simulates values >80% (Fig. 5g). Alternatively, Group 1 is colder than Group 2 in the most frequently occurring bins (Fig. 10f) and this could lead to differences in cloud microphysics and ice formation. Inter-model differences

**Deleted:** -

**Deleted:** -

in *SHF* and *LHF* indicate that the intergroup differences change sign with increasing *LTS*; however, these differences anti-correlate with the intergroup differences in low cloud amount.

Intergroup differences in cloud microphysics and specifically the production of cloud liquid versus ice strongly corresponds to intergroup differences in low cloud amount. Figure 11 illustrates the differences in lower tropospheric *CLW* (Fig. 11 a-c), *CLI* (Fig. 11 d-f), and ice condensate fraction, (*ICF*; Fig. 11 g-i) stratified by *LTS* and $-\omega_{500}$. Ice condensate fraction is defined as cloud ice water mixing ratio (*CLI*) divided by total cloud condensate mixing ratio (*CLI+CLW*). Results for summer are presented in Figure 12. Both groups exhibit similar overall dependencies of the liquid and ice water mixing ratio on *LTS* and $-\omega_{500}$ with Group 2 producing more cloud liquid than Group 1 (Fig. 11c) and slightly more cloud ice (Fig. 11f). The ICF, however, (Fig. 11g,h) indicates that Group 1 produces a much higher percentage of total condensate as ice (*ICF* greater than 0.5 in the most frequently occurring regimes). Figures 11 and 12 support the idea that Group 1 models sustain a larger fraction of thin ice clouds at cold temperatures supporting larger low cloud amount in winter. Moreover, the finding that Group 1 models are drier than Group 2 suggests that the enhanced cloud ice formation dehydrates the winter Arctic atmosphere in these models. The smaller *CLW* in Group 1 may also be related to the greater *CLI* as some models do not allow supersaturation with respect to ice meaning that liquid supersaturation would not be reached under most Arctic winter conditions. This result is consistent with the Kretzschmar et al. (2018) result showing that not allowing ice supersaturation corresponds to a positive bias in low cloud cover in ECHAM6. Alternatively, the larger production of cloud liquid by Group 2 corresponds to a larger low cloud amount in summer. The correspondence between the larger production of cloud liquid and larger low cloud fraction in summer relates to warmer temperatures being less favorable for cloud ice formation. The results support the argument that cloud phase partitioning and cloud

**Deleted:** and

**Deleted:**

**Deleted:** (

**Deleted:** .

**Formatted:** Font: Not Italic, Not Superscript/ Subscript

**Formatted:** Font: Not Italic

**Deleted:** ratio of cloud ice to total condensate

**Deleted:** predominantly ice clouds and mixed-phase clouds with large fractions of ice condensate

**Deleted:** while Group 2 clouds are mixed-phase

**Deleted:** Intergroup differences clearly show that Group 2 models produce more cloud liquid whereas Group 1 models produce more ice; Fig. 12 illustrates that same results in summer.

**Formatted:** Font: Not Italic, Not Superscript/ Subscript

**Deleted:** our

**Formatted:** Not Highlight

**Deleted:** production

**Deleted:** ice

**Deleted:** is

microphysical parameterizations explain the differences in the Arctic cloud amount annual cycle and differences in the surface turbulent fluxes and atmospheric circulation contribute little. Therefore, improved representation of the Arctic cloud amount annual cycle requires improvements in the representation of cloud microphysical processes in low clouds.

To investigate the role of microphysics further we set out to stratify the models into new groups based upon whether or not supersaturation with respect to ice was allowed. However, we cannot because the information about to whether a particular model allows ice supersaturation or not was not consistently identified in the citing literature (Table 1). Sufficient detail is provided in the literature to partition the models into Group A those that treat cloud ice and water as prognostic variables and Group B those that treat total water as a prognostic variable and use a temperature-dependent phase partitioning. Figure 13 illustrates the joint distributions of low cloud amount, CLW, CLI, and ICF in DJF. While Groups A and B both contain Groups 1 and 2 models, the distributions of CLW, CLI, and ICF in Fig. 13 resembles that shown in Fig. 11. The results indicate that models treating total cloud water as a prognostic variable and use a temperature-dependent phase partitioning have a smaller ice condensate fraction (less cloud ice and more cloud water) than those that treat cloud ice and liquid prognostically. The cloud fraction differences between this microphysical scheme-based grouping is less than the original group while taking on the same shape. Thus, this result supports the argument that the cloud microphysical treatment is the principle factor explaining the differences in the intergroup low cloud amount differences.

Due to the importance of $T_A$ and $RH$ to this explanation, we further investigate the low cloud amount dependence on $T_A$ and $RH$ as both variables influence the cloud microphysics parameterizations. Figures 14 and 15 illustrate the joint distribution of the average low cloud amount stratified by lower tropospheric $T_A$ and $RH$ and frequency of occurrence of each bin in

**Formatted:** Not Highlight
**Formatted:** Not Highlight
**Formatted:** Not Highlight
**Formatted:** Not Highlight
**Formatted:** Not Highlight
**Formatted:** Not Highlight
**Formatted:** Not Highlight
**Formatted:** Not Highlight
**Formatted:** Not Highlight
**Formatted:** Not Highlight
**Formatted:** Not Highlight
**Formatted:** Font: Times
**Formatted:** Font: Times
**Formatted:** Font: Times
**Formatted:** Not Highlight
**Formatted:** Font: Times
**Formatted:** Not Highlight
**Formatted:** Font: Times
**Formatted:** Not Highlight
**Formatted:** Font: Times
**Formatted:** Font: Times
**Formatted:** Font: Times
**Formatted:** Font: Times
**Formatted:** Font: Times
**Formatted:** Not Highlight
**Formatted:** Font: Times
**Formatted:** Not Highlight
**Formatted:** Font: Times
**Deleted:** ¶
**Deleted:** 3
**Deleted:** 4

winter and summer, respectively. The largest intergroup differences are found at the coldest temperatures and highest *RH* values for both winter (Fig. 14) and summer (Fig. 15). Group 1 favors cooler and drier atmospheric conditions than Group 2 (Fig. 14c), while also producing more clouds under those conditions. In summer, Group 2 models produce larger low cloud amounts compared to Group 1 in the warmer and more humid conditions occurring most frequently (Fig. 15). Group 2 also slightly favors more humid conditions in summer than Group 1 contributing to larger summer low cloud amount. Results applying the decomposition from (1) to the $T_A$ and *RH* joint distribution indicate that in winter differences in the parameterized cloud physics are primarily responsible for $\delta LCA_{G1-G2}$, where as in summer the relative frequency of occurrence is primarily responsible for $\delta LCA_{G1-G2}$ (Table 4). This result supports our conclusion that cloud microphysical processes explain the model differences in Arctic low cloud amount in winter. In summer, however, Fig. 15 indicates that processes that control the frequency of occurrence of $T_A$ and *RH* states are also important to explain low cloud amount differences.

4. Discussion

This analysis explores the factors that influence Arctic cloud amount within contemporary climate models with the specific focus on understanding the factors that drive differences in the Arctic cloud amount annual cycle. In comparing our results with previous work, the vertically-resolved cloud amount dependencies (Figs. 6 and 7) on cloud influencing factors agrees with the observationally-based analysis of Li et al. (2014). It should be noted that this result is despite differences in the temporal characteristics of the two analyses: monthly-averaged model output vs. instantaneous satellite data. This result suggests that the use of monthly averages is not as big of a limiting factor for investigating the cloud dependence on atmospheric and surface conditions as previously assumed. Our results demonstrate that climate model physical parameterizations

**Deleted:** 3

**Deleted:** 4

**Deleted:** 3

**Deleted:** 4

**Formatted:** Font: Italic

**Formatted:** Font: Italic, Subscript

**Formatted:** Font: Italic

**Deleted:** 3

**Deleted:** 4

**Deleted:** TA and RH

**Deleted:** implies

realistically reproduce the general Arctic cloud amount dependence on atmospheric condition, yet subtle differences produce large discrepancies in the Arctic cloud amount annual cycle between models and between models and observations. While a thorough model-observation comparison using CALIPSO-CloudSAT satellite simulator output is the subject of ongoing work, our results indicate that neither Group 1 or 2 reproduces observations (Fig. 3). Individual models significantly outperform the Group 1 and 2 averages as indicated by the close proximity of five models (bcc-csm1-1, CMCC-CM, CanESM2, MPI-ESM-MR, and MPI-ESM-LR) to the observations (denoted by stars) in Fig. 2.

We argue that the primary cause of the larger cloud amount in Group 1 during winter is due to the production and maintenance of low, thin ice clouds at colder surface air temperatures than Group 2. We hypothesize that Group 1 maintains low cloud amount at colder temperatures as a result of ice microphysical parameterization differences by maintaining a larger fraction of cloud ice than Group 2 overall and especially at colder temperatures and lower *RH* (Fig. S4g-i illustrates the *ICF* stratified by *RH* and *T*). This hypothesis seems at odds with previous cloud process research considering the mixed-phase cloud system where high cloud ice production desiccates super cooled liquid and more efficiently precipitates reducing low cloud amount (e.g., Avramov et al. 2011; Morrison et al. 2012). In this case, the results suggest that Group 1 overcomes this by producing more cloud ice. In addition, we do not know the frequency of mixed-phase clouds from monthly averaged output. Overall, the importance of cloud microphysics to model cloud amounts is consistent with previous work illustrating that Arctic clouds and their radiative effects strongly respond to changes in ice microphysics (English et al. 2014; Pithan et al. 2014; Tan and Storelvmo 2016; McCoy et al. 2016; Kay et al. 2016).

**Deleted:** differences

**Formatted:** Font: Times

**Deleted:** .

**Formatted:** Font: Times

**Formatted:** Font: Times

**Deleted:**

**Deleted:** producing

**Deleted:** more

**Deleted:** , Pithan et al. 2014

What do our results argue about the drivers of the Arctic cloud annual cycle? The climate model results argue that the Arctic cloud annual cycle is most strongly driven by the seasonality of cloud microphysics, specifically the cloud phase and temperature relationship. The *SIC* in both the inter-group differences as well as the cloud amount dependence on sea ice shows a weaker relationship than the other factors indicating a limited role in driving the Arctic cloud annual cycle. The results do not support a significant role for the seasonality of relative humidity in forcing the Arctic low cloud annual cycle because (1) the seasonality of *RH* is similar between the two groups (Fig. S3) and (2) models that produce fewer winter clouds possess higher *RH*. Rather, the cloud microphysics appear to shape Arctic lower tropospheric *RH*. Changes in atmospheric conditions, specifically *LTS* and $-\omega_{500}$, are significant between winter and summer indicating a role for the large-scale circulation. Our results support the idea of Beesley and Moritz (1999) that the covariance between atmospheric temperature and cloud microphysics is a major factor responsible for the Arctic cloud annual cycle.

A critical consideration is the cloud ice formation process. Models that do not allow supersaturation with respect to ice implicitly assume that deposition freezing is the dominant ice formation process in Arctic low clouds. However, observational evidence indicates that supercooled liquid must first be present before cloud ice is observed at temperatures warmer than -25°C, supporting the notion that immersion freezing is the dominant ice nucleation process (de Boer et al. 2011). Our results indicate that a better understanding of ice formation mechanisms operating in the Arctic and the conditions under which each dominates would provide an important constraint on climate model physics and Arctic climate simulations.

A new idea from this analysis is one of Arctic cloud susceptibility. Returning to the *LTS* and $-\omega_{500}$ joint distributions, summer versus winter differences (Figs. 8a,b, and 9a,b) in the low

**Formatted:** Font: Italic

**Deleted:** also

**Formatted:** Font: Italic

**Formatted:** Font: Italic

**Formatted:** Font: Italic

**Formatted:** Font: Italic

**Formatted:** Font: Italic

**Formatted:** Font: Italic

**Formatted:** Font: Italic

cloud amount dependence are significant. Figures 8 and 9 show that the most frequently occurring atmospheric conditions in summer are found along a strong gradient in the low cloud amount dependence on *LTS* and $-\omega_{500}$, not the case for winter. This suggests that summer low cloud amount is more susceptible to changes in atmospheric conditions than winter low clouds. This apparent difference in the susceptibility of low cloud amount to changes in atmospheric conditions could have important implications for Arctic cloud feedback, as Taylor (2017) illustrates that changes in *LTS* imply large changes in the surface cloud radiative effect.

## 5. Conclusion

Surface and space-based observations of Arctic clouds exhibit a robust annual cycle with maximum cloud amount in fall and a minimum in winter. Variations in cloud amount affect energy flows in the Arctic and strongly influence the surface energy budget. Therefore, understanding the role of clouds in the context of the present-day Arctic climate is imperative for improving predictions of surface temperature and sea ice variability, as well as for projecting Arctic climate change. As we and several authors before demonstrate, contemporary climate models struggle to reproduce the observed Arctic cloud amount and its variability, especially within the context of the annual cycle.

Our analysis focuses on identifying the causes of the climate model differences in the annual cycle representation. We find that most climate models tend to fall into one of two groups: one favoring larger winter cloud amount and another favoring larger summer cloud amount. The results demonstrate that differences in low, thin ice clouds at pressures >950 hPa, not middle or high clouds, are primarily responsible for the total cloud amount annual cycles within each group. These discrepancies between the two model groups exhibit little spatial variability, are consistent between land and ocean, and are only weakly influenced by sea ice concentration, suggesting that the cause of the cloud amount differences operates Arctic-wide.

Differences in atmospheric and surface conditions represent an important potential source of the low cloud amount differences. The results show small differences in the annual, domain-averaged atmospheric and surface conditions between the two groups and indicate that these are not responsible for the low cloud amount differences. Considering specific atmospheric and surface conditions, we find that models disagree most under strong lower tropospheric stability, weak to moderate mid-tropospheric subsidence, and cold lower tropospheric air temperatures. Overall, the cloud amount dependence on cloud influencing factors explains most of the inter-group differences in cloud amount. Since, the cloud amount dependence on cloud influencing factors in climate models is governed by parameterized cloud physics, the results indicate that parameterization differences are responsible for the cloud amount discrepancies and that differences in the frequency of occurrence of atmospheric and surface conditions between the models is not a significant factor.

Why do models simulate different low cloud amounts under specific atmospheric conditions? Models produce similar dependencies of low cloud amount on atmospheric and surface conditions in summer but not in winter. Models able to sustain larger low cloud amounts at colder surface air temperatures simulate more winter clouds and we argue that the details of the ice microphysical parameterization are responsible by maintaining a larger fraction of cloud ice in some models than others. The present analysis is unable to isolate the specific characteristics of the ice microphysical parameterization (e.g., ice formation, crystal habit, mass-diameter relationship, fall speed, gamma size distribution parameters, etc.) that drive these differences, however this should be the focus of

**Deleted:** causing

**Deleted:** production

future investigation. A commonality of these ice microphysical parameterization characteristics is that few observational constraints are available.

Our results have several implications to our understanding of the Arctic climate system and for modeling.

- Cloud ice microphysical processes are important contributors to the Arctic low cloud amount annual cycle and therefore are important to the seasonality of the Arctic surface energy budget and sea ice cover.
- Mean Arctic low cloud amount is strongly constrained by atmospheric variability, namely by the lower tropospheric stability and mid-tropospheric vertical motion fields.
- Lower tropospheric stability plays an important role in explaining the inter-model differences in low cloud amount.
- Cloud microphysical parameterizations drive significant inter-model differences in Arctic cloud amount and its annual cycle.
- Improved modeling of the Arctic cloud amount annual cycle, and its influences on Arctic climate variability and change, requires observational constraints on ice microphysical processes, particularly on cloud phase partitioning and ice formation mechanisms.
- The general thinking that models producing too much ice then desiccate supercooled liquid and yield fewer clouds does not explain model biases in low cloud amount. Our results indicate that in winter a larger ice condensate fraction supports larger low cloud amounts, likely because models simulate very little supercooled liquid in winter. Larger supercooled liquid water is associated with larger low cloud amounts in summer.

**Deleted:** production

- Lastly, we were surprised to find that models treating cloud ice and liquid condensate as separate prognostic variables simulate larger ice condensate fractions than those that treat total cloud condensate as a prognostic variable and use a temperature-dependent phase partitioning.

In closing, Arctic cloud amount plays a significant role in shaping Arctic climate system evolution. Given the stark evidence that the Arctic climate is changing more rapidly than the rest of the globe, improved modeling capabilities in this highly varying, highly susceptible, and geopolitically important region is urgent. A better understanding of Arctic clouds is vital to providing this improved capability. This analysis advances our understanding of the factors that drive Arctic cloud behavior in climate models and points to unresolved issues in ice microphysics as the likely explanation. Thus, our results underscore the vital need for observational constraints on these critical processes.

## References

Barton, N. P., S.A. Klein, J. S. Boyle, and Y. Y. Zhang, 2012: Arctic synoptic regions: Comparing domain-wide Arctic cloud observations with CAM4 and CAM5 during similar dynamics, *J. Geophys. Res.*, **117**, doi:10.1029/2012JD017589.

Beeseley, J. A. and R. E. Moritz, 1999: Toward an explanation of the annual cycle of cloudiness over the Arctic Ocean. *J. Climate*, **12**, 395-415.

Boeke, R. C. and P. C. Taylor, 2016: Evaluation of the Arctic surface radiation budget in CMIP5 models. *J. Geophys. Res.*, **121**, 8525-8548, doi: 10.1002/2016JD025099.

Bosilovich, M. G. and coauthors, 2015: MERRA-2: *Initial Evaluation of the Climate*. NASA Technical Report SERES on Global Modeling and Data Assimilation Volume 43. 139 pages.

Cesana, G., J. E. Kay, H. Chepfer, J. M. English, and G. de Boer, 2012: Ubiquitous low-level liquid-containing Arctic clouds: New observations and climate model constraints form CALIPSO-GOCCP. *Geophys. Res. Lett.*, **39**, L20804, doi:10.1029/2012GL053385.

Coopman, Q., Garrett, T. J., Finch, D. P., and Riedi, J., 2018: High sensitivity of arctic liquid clouds to long-range anthropogenic aerosol transport. *Geophys. Res. Lett.*, **45**, 372–381. https://doi.org/10.1002/2017GL075795.

Hahn, C. J., Warren, S. G., and London, J., 1995: The effect of moonlight on observation of cloud cover at night, and application to cloud climatology. *J. Climate*, **8**, 1429–1446.

Hegyi, B. M. and P. C. Taylor, 2017: The Arctic Oscillation and Arctic Dipole regionally influence the wintertime surface radiation budget. *Geophys. Res. Lett.* **44**, doi: 10.1002/2017GL073281.

Huschke, R., 1969: Arctic cloud statistics from ‘‘air-calibrated’’ surface weather observations. The Rand Corp., 79 pp.

Jackson, R. C., G. M. McFarquhar, A. V. Korolev, M. E. Earle, P. S. K. Liu, R. P. Lawson, S. Brooks, M. Wolde, A. Laskin, and M. Freer, 2012: The dependence of ice microphysics on aerosol concentration in arctic mixed-phase stratus clouds during ISDAC and M-PACE. *J. Geophys. Res.*, **117**, D15207, doi:10.1029/2012JD017668.

Kretzschmar, J., Salzmann, M., Mülmenstädt, J., and Quaas, J.: Arctic cloud cover bias in ECHAM6 and its sensitivity to cloud microphysics and surface fluxes, *Atmos. Chem. Phys. Discuss.*, https://doi.org/10.5194/acp-2018-1135, in review, 2018.

Liu, Y. and J. R. Key, 2016: Assessment of Arctic cloud cover anomalies in atmospheric reanalysis products using satellite data. *J. Climate*, **29**, 6065-6083, doi: 10.1175/JCLI-D-15-0861.1.

**Formatted:** Font: Italic

**Formatted:** Font color: Text 1

Liu, Y. M. D. Shupe, Z. Wang, and G. Mace, 2017: Cloud vertical distribution from combined surface and space radar-lidar observations at two Arctic atmospheric observatories. *Atmos. Chem. Phys.,* **17**, 5973-5989, doi: 10.5194/acp-17-5973-2017.

Pithan, F., B. Medeiros, T. Mauritsen, 2014: Mixed-phase clouds case climate model biases in Arctic wintertime temperature inversions. *Clim. Dyn.*, **43**, 289-303.

Taylor, P. C., 2017: Does the relationship between Arctic low clouds and sea ice matter? Current Problems in Atmospheric Radiation (IRS 2016): AIP Conference Proceedings **1810**, 070009, doi: http://dx.doi.org/10.1063/1.4975530.

Taylor, P. C., S. Kato, K.-M. Xu, and M. Cai, 2015: Covariance between Arctic sea ice and clouds within atmospheric state regimes at the satellite footprint level. *J. Geophys. Res. Atmos.*, **120**, 12656-12678, doi:10.1002/2015JD023520.

List of Tables

List of Figures



**Deleted:** Fig. 1. Annual cycle of (a) total cloud amount, (b) low cloud amount (defined as cloud between 1000 – 850 hPa) and (c) high cloud amount (cloud between 500 – 300 hPa). Color lines represent individual CMIP5 models. The black line with squares represents C3M observations and the black line with circles represents MERRA-2. The gray shading in (a) represents the 95% confidence interval for the difference in means between C3M and the ensemble; the... [1]

**Deleted:** Fig. 2: Average winter (DJF) cloud fraction vs... [2]

**Deleted:** Fig. 3. Vertically-resolved mean cloud amount... [3]

**Formatted:** Font: Italic

**Formatted:** Font: Italic

**Formatted:** Font: Italic

**Formatted:** Font: Italic

**Formatted:** Font: Italic

**Formatted:** Font: Italic

**Formatted:** Font: Italic

**Formatted:** Font: Italic

**Formatted:** Font: Italic

**Formatted:** Font: Italic

**Deleted:** Fig. 5. Probability distributions of (a) LTS, (b) -ω... [4]

**Formatted:** Font: Italic

**Formatted:** Font: Italic

**Formatted:** Font: Italic

**Formatted:** Font: Italic

**Formatted:** Font: Italic

**Formatted:** Font: Italic

**Formatted:** Font: Italic

**Formatted:** Font: Italic

**Formatted:** Font: Italic

**Formatted:** Font: Italic

**Formatted:** Font: Italic

**Formatted:** Font: Italic

**Formatted:** Font: Italic

**Formatted:** Font: Italic

**Formatted:** Font: Italic

**Formatted:** Font: Italic

**Formatted:** Font: Italic

**Formatted:** Font: Italic

**Formatted:** Font: Italic

**Formatted:** Font: Italic

**Formatted:** Font: Italic

Fig. 9. Contours of average low cloud amount for summer in a *LTS*/-$\omega_{500}$ joint distribution for (a) Group 1, (b) Group 2, and (c) Group 1 minus Group 2. The frequency of occurrence each *LTS*/-$\omega_{500}$ interval is contoured in black for Group 1 (a), Group 2 (b), and the difference in frequency of occurrence (c). In (c), the solid contouring represents regimes occurring more frequently in Group 1 while the dashed contouring are those regimes occurring more frequently in Group 2.

Fig. 10. Contours of DJF atmospheric and surface conditions in the *LTS* and -$\omega_{500}$ joint distribution for (left column) Group 1, (middle column) Group 2, and (right column) Group 1 minus Group 2 for (a-c) *RH*, (d-f) $T_A$ at 950hPa, (g-l) *SHF*, and (j-l) *LHF*.

Fig. 11. Contours of winter low cloud liquid water mixing ratio for (a) Group 1, (b) Group 2, and (c) Group 1 minus Group 2 and low cloud ice water mixing ratio (d) Group 1, (e) Group 2, and (f) Group 1 minus Group 2. Ice condensate fraction is shown in the bottom panels for Group 1 (g), Group 2 (h), and Group 1 minus Group 2 (i).

Fig. 12. Contours of summer low cloud liquid water mixing ratio for (a) Group 1, (b) Group 2, and (c) Group 1 minus Group 2 and low cloud ice water mixing ratio (d) Group 1, (e) Group 2, and (f) Group 1 minus Group 2. Ice condensate fraction is shown in the bottom panels for Group 1 (g), Group 2 (h), and Group 1 minus Group 2 (i).

Fig. 13. Contours of winter low cloud amount for (a) Group A, (b) Group B, and (c) Group A minus Group B, low liquid water mixing ratio (d) Group A, (e) Group B, and (f) Group A minus Group B, low cloud ice water mixing ratio Group A (g), Group B (h), and Group A minus Group B (i). and ice condensate fraction is shown in the bottom panels for Group A (j), Group B (k), and Group A minus Group B (l).

Fig. 14. Contours of average low cloud amount for winter in a $T_A$-*RH* joint distribution for (a) Group 1, (b) Group 2, and (c) Group 1 minus Group 2. The frequency of occurrence each $T_A$-*RH* interval is contoured in black for Group 1 (a), Group 2 (b), and the difference in frequency of occurrence (c).

Fig. 15. Contours of average low cloud amount for summer in a $T_A$-*RH* joint distribution for (a) Group 1, (b) Group 2, and (c) Group 1 minus Group 2. The frequency of occurrence each $T_A$-*RH* interval is contoured in black for Group 1 (a), Group 2 (b), and the difference in frequency of occurrence (c).

**Deleted:** Fig. 8. Contours of average low cloud amount for DJF in the LTS and -$\omega_{500}$ joint distribution for (a) Group 1, (b) Group 2, and (c) Group 1 minus Group 2 and the frequency of occurrence each LTS and -$\omega_{500}$ interval for (d) Group 1, (e) Group 2, and (f) Group 1 minus Group 2.¶

**Deleted:** Fig. 9. Contours of average low cloud amount for JJA in the LTS and -$\omega_{500}$ joint distribution for (a) Group 1, (b) Group 2, and (c) Group 1 minus Group 2 and the frequency of occurrence each LTS and -$\omega_{500}$ interval for (d) Group 1, (e) Group 2, and (f) Group 1 minus Group 2.¶

**Formatted:** Font: Italic

**Formatted:** Font: Italic

**Formatted:** Font: Italic

**Formatted:** Font: Italic

**Formatted:** Font: Italic

**Formatted:** Font: Italic

**Formatted:** Font: Italic

**Formatted:** Font: Italic

**Deleted:** Fig. 11. Contours of DJF low cloud CLW for (a) Group 1, (b) Group 2, and (c) Group 1 minus Group 2 and CLI (d) Group 1, (e) Group 2, and (f) Group 1 minus Group 2.¶

**Deleted:** ¶

**Deleted:** Fig. 12. Contours of JJA low cloud CLW for (a) Group 1, (b) Group 2, and (c) Group 1 minus Group 2 and CLI (d) Group 1, (e) Group 2, and (f) Group 1 minus Group 2.¶

**Deleted:** 3

**Deleted:** Fig. 13. Contours of average low cloud amount for DJF the TA-RH joint distribution for (a) Group 1, (b) Group 2, and (c) Group 1 minus Group 2 and the frequency of occurrence of each TA-RH interval for (d) Group 1, (e) Group 2, and (f) Group 1 minus Group 2.¶

**Deleted:** 4

Table 1: Outline of cloud and microphysics schemes for CMIP5 models used in this study

| Model | Institution | Cloud Fraction and Microphysics | Reference |
|---|---|---|---|
| ACCESS1.0 | Commonwealth Scientific and Industrial Research Organisation, Bureau of Meteorology | PDF-based diagnostic cloud scheme with bulk single moment microphysics | *Collier and Uhe* [2012]; *Bi et al.* [2012a] |
| ACCESS1.3 | Commonwealth Scientific and Industrial Research Organisation, Bureau of Meteorology | PDF-based prognostic cloud scheme with bulk single moment microphysics | *Collier and Uhe* [2012]; *Bi et al.* [2012a] |
| BCC-CSM1.1 | Beijing Climate Center | non-PDF prognostic cloud scheme, bulk single moment microphysics | *Wu et al.* [2008] |
| BCC-CSM1.1(m) | Beijing Climate Center | non-PDF prognostic cloud scheme, bulk single moment microphysics | *Wu et al.* [2008] |
| BNU-ESM | College of Global Change and Earth System Science, Beijing Normal University | non-PDF diagnostic cloud fraction with prognostic cloud water, bulk single moment microphysics | *Ji et al.* [2014]; *Wu et al.* [2013] |
| CanESM2 | Canadian Centre for Climate Modelling and Analysis | PDF-based diagnostic cloud scheme with bulk single moment microphysics | *Arora et al.* [2011]; *von Salzen et al.* [2013] |
| CCSM4 | National Center for Atmospheric Research | non-PDF diagnostic cloud fraction with prognostic cloud water, bulk single moment microphysics | *Gent et al.* [2011]; *Gettelman et al.* [2008] |
| CMCC-CM | Centro Euro-Mediterraneo per I Cambiamenti Climatici | PDF-based prognostic cloud scheme, double moment microphysics | *www.cmcc.it/models/cmcc-cm; Roeckner et al. [2003]* |
| CESM1-BGC | National Science Foundation, Dept. of Energy, National Center for Atmospheric Research | non-PDF diagnostic cloud fraction with prognostic cloud water, bulk single moment microphysics | *Gent et al.* [2011] |
| CESM1-CAM5 | National Science Foundation, Dept. of Energy, National Center for Atmospheric Research | Prognostic two-moment formulation of cloud liquid and ice with mass and number concentration . Multiple ice nucleation mechanisms calculated; allows for supersaturation with respect to ice | *Neale, R. et al.* [2012]; *Meehl et al.* [2013]; *Gettelman et al. 2008* |
| CNRM-CM5 | Centre National de Recherches Meteorologiques, Centre Europeen de Recherche et Formation Avancees en Calcul Scientifique | PDF-based diagnostic cloud scheme | *Voldoire et al.* [2012] |
| CSIRO-Mk3.6.0 | Commonwealth Scientific and Industrial Research Organisation in collaboration with the Queensland Climate Change Centre of Excellence | non-PDF diagnostic cloud scheme, bulk single moment microphysics | *Rotstayn et al.* [2012] |
| FGOALS-g2 | LASG, Institute of Atmospheric Physics, Chinese Academy of Sciences; and CESS, Tsinghua University | non-PDF cloud scheme, 2-moment microphysics | *Li et al.* [2013] |
| GFDL-CM3 | Geophysical Fluid Dynamics Laboratory | PDF-based prognostic cloud scheme, bulk single moment microphysics | *Donner et al.* [2011] |
| GISS-E2-H | NASA Goddard | non-PDF diagnostic cloud scheme, bulk single moment microphysics | *Menon et al.* [2010]; *Del Genio* [1996] |
| GISS-E2-R | NASA Goddard | non-PDF diagnostic cloud scheme, bulk single moment microphysics | *Menon et al.* [2010]; Del Genio [1996] |
| INM-CM4 | Institute for Numerical Mathematics | non-PDF diagnostic cloud scheme, bulk single moment microphysics | *Volodin, Diansky, and Gusev* [2010] |
| IPSL-CM5A-LR | Institut Pierre-Simon Laplace | PDF-based diagnostic cloud scheme with bulk single moment microphysics | *Dufresne et al.* [2013] |
| IPSL-CM5A-MR | Institut Pierre-Simon Laplace | PDF-based diagnostic cloud scheme with bulk single moment microphysics | *Dufresne et al.* [2013] |
| MIROC5 | Atmosphere and Ocean Research Institute (The University of Tokyo), National Institute for Environmental Studies, Japan Agency for Marine-Earth Science and Technology | PDF-based prognostic cloud scheme with bulk single moment microphysics | *Watanabe et al. [2010*] |
| MPI-ESM-MR | Max Planck Institute for Meteorology | PDF-based diagnostic cloud fraction | *Raddatz et al.* [2007] |
| MPI-ESM-LR | Max Planck Institute for Meteorology | PDF-based diagnostic cloud fraction | *Raddatz et al.* [2007] |
| MRI-CGCM3 | Meteorological Research Institute | PDF-based diagnostic cloud scheme with double moment microphysics | *Yukimoto et al.* [2011] |
| NorESM1-M | Norwegian Climate Centre | non-PDF diagnostic cloud fraction with prognostic cloud water, bulk single moment microphysics | *Kirkevag et al.* [2013]; *Rasch and Kristjansson* [1998] |
| NorESM1-ME | Norwegian Climate Centre | non-PDF diagnostic cloud fraction with prognostic cloud water, bulk single moment microphysics | *Kirkevag et al.* [2013]; Rasch and Kristjansson [1998] |

**Deleted:** Fig. 14. Contours of average low cloud amount for JJA the TA-RH joint distribution for (a) Group 1, (b) Group 2, and (c) Group 1 minus Group 2 and the frequency of occurrence of each TA-RH interval for (d) Group 1, (e) Group 2, and (f) Group 1 minus Group 2.

Column Break

Table 2. Annual mean atmospheric conditions for MERRA-2, Group 1, Group 2 for ocean and land, and the 95% confidence interval for the difference in means (Group 1 – Group 2).

**OCEAN**

| | MERRA-2 | GROUP 1 | GROUP 2 | 95% CI OF $\mu_{G1} - \mu_{G2}$ |
|---|---|---|---|---|
| **LTS (K)** | 20.76 | 20.75 | 23.30 | $-2.55 < \mu_{G1}-\mu_{G2} < -2.54$ |
| **$-\omega_{500}$ (hPa day$^{-1}$)** | 1.16 | 0.90 | -0.33 | $1.21 < \mu_{G1}-\mu_{G2} < 1.24$ |
| **SHF (W m$^{-2}$)** | 12.33 | 4.55 | 5.69 | $-1.167 < \mu_{G1}-\mu_{G2} < -1.119$ |
| **LHF (W m$^{-2}$)** | 13.78 | 11.85 | 10.23 | $1.59 < \mu_{G1}-\mu_{G2} < 1.64$ |
| **LOW CLOUD (%)** | 24.20 | 25.60 | 22.66 | $2.938 < \mu_{G1}-\mu_{G2} < 2.96$ |
| **HIGH CLOUD (%)** | 16.80 | 18.00 | 12.65 | $5.35 < \mu_{G1}-\mu_{G2} < 5.36$ |
| **SIC (%)** | | 76.60 | 81.30 | $-4.71 < \mu_{G1}-\mu_{G2} < -4.64$ |
| **LOW-LEVEL RH (%)** | 84.00 | 79.50 | 85.20 | $-5.72 < \mu_{G1}-\mu_{G2} < -5.70$ |
| **LOW-LEVEL $T_A$ (K)** | 262.50 | 260.90 | 260.90 | $-0.008 < \mu_{G1}-\mu_{G2} < 0.0097$ |
| **CLI (g kg$^{-1}$)** | 0.0016 | 0.0050 | 0.0043 | $0.00074 < \mu_{G1}-\mu_{G2} < 0.00075$ |
| **CLW (g kg$^{-1}$)** | 0.0197 | 0.0140 | 0.0246 | $-0.0105 < \mu_{G1}-\mu_{G2} < -0.0104$ |

**LAND**

| | MERRA-2 | GROUP 1 | GROUP 2 | 95% CI OF $\mu_{G1} - \mu_{G2}$ |
|---|---|---|---|---|
| **LTS (K)** | 20.48 | 19.90 | 21.30 | $-1.315 < \mu_{G1}-\mu_{G2} < -1.29$ |
| **$-\omega_{500}$ (hPa day$^{-1}$)** | -2.95 | -3.73 | -0.48 | $-3.287 < \mu_{G1}-\mu_{G2} < -3.2$ |
| **SHF (W m$^{-2}$)** | 1.79 | 0.74 | 2.20 | $-1.48 < \mu_{G1}-\mu_{G2} < -1.425$ |
| **LHF (W m$^{-2}$)** | 21.10 | 15.32 | 13.50 | $1.78 < \mu_{G1}-\mu_{G2} < 1.83$ |
| **LOW CLOUD (%)** | 15.10 | 22.67 | 20.50 | $2.148 < \mu_{G1}-\mu_{G2} < 2.175$ |
| **HIGH CLOUD (%)** | 17.30 | 21.15 | 14.7 | $6.40 < \mu_{G1}-\mu_{G2} < 6.42$ |
| **LOW-LEVEL RH (%)** | 80.80 | 76.50 | 82.60 | $-6.12 < \mu_{G1}-\mu_{G2} < -6.09$ |
| **LOW-LEVEL $T_A$ (K)** | 265.30 | 263.90 | 263.60 | $0.267 < \mu_{G1}-\mu_{G2} < 0.293$ |
| **CLI (g kg$^{-1}$)** | 0.0008 | 0.0045 | 0.0049 | $-0.00034 < \mu_{G1}-\mu_{G2} < -0.00032$ |
| **CLW (g kg$^{-1}$)** | 0.0174 | 0.0160 | 0.0276 | $-0.0115 < \mu_{G1}-\mu_{G2} < -0.0114$ |

**Deleted:** 1

**Deleted:** *<object>*

Table 3. Summary of the average low cloud amount for each group from model output and as computed using Equation (1).

| | GROUP 1 | GROUP 2 |
|---|---|---|
| DJF domain-averaged LCA | 29.0% | 17.2% |
| DJF LCA from predictive model | 29.8% | 16.3% |
| JJA domain-averaged LCA | 23.1% | 27.0% |
| JJA LCA from predictive model | 21.8% | 26.1% |

Deleted: 2

Deleted: ¶
[Robyn please insert text table]

Table 4. Summary of decomposition results attributing Group 1 minus Group 2 differences in the average low cloud amount following Equation (2).

**AVERAGE LCA CONSTRUCTED FROM [$LTS_i$, $-\omega_{500,j}$]**

| | $\overline{\Delta LCA}_{G1-G2}$ | $\overline{\delta LCA}_{G1-G2}$ | $\delta LCA_{G1-G2} \cdot RFO_{G1}$ | $LCA_{G1} \cdot \delta RFO_{G1-G2}$ |
|---|---|---|---|---|
| **WINTER** | 11.80% | 13.30% | 13.10% | 0.17% |
| **SUMMER** | -3.84% | -4.45% | -4.49% | 0.05% |

**AVERAGE LCA CONSTRUCTED FROM [$T_{a,i}$, $RH_j$]**

| | $\overline{\Delta LCA}_{G1-G2}$ | $\overline{\delta LCA}_{G1-G2}$ | $\delta LCA_{G1-G2} \cdot RFO_{G1}$ | $LCA_{G1} \cdot \delta RFO_{G1-G2}$ |
|---|---|---|---|---|
| **WINTER** | 11.60% | 10.40% | 12.20% | -1.80% |
| **SUMMER** | -4.20% | -4.68% | -1.37% | -3.31% |

**Deleted:** 3

**Deleted:** [Robyn please insert text table]

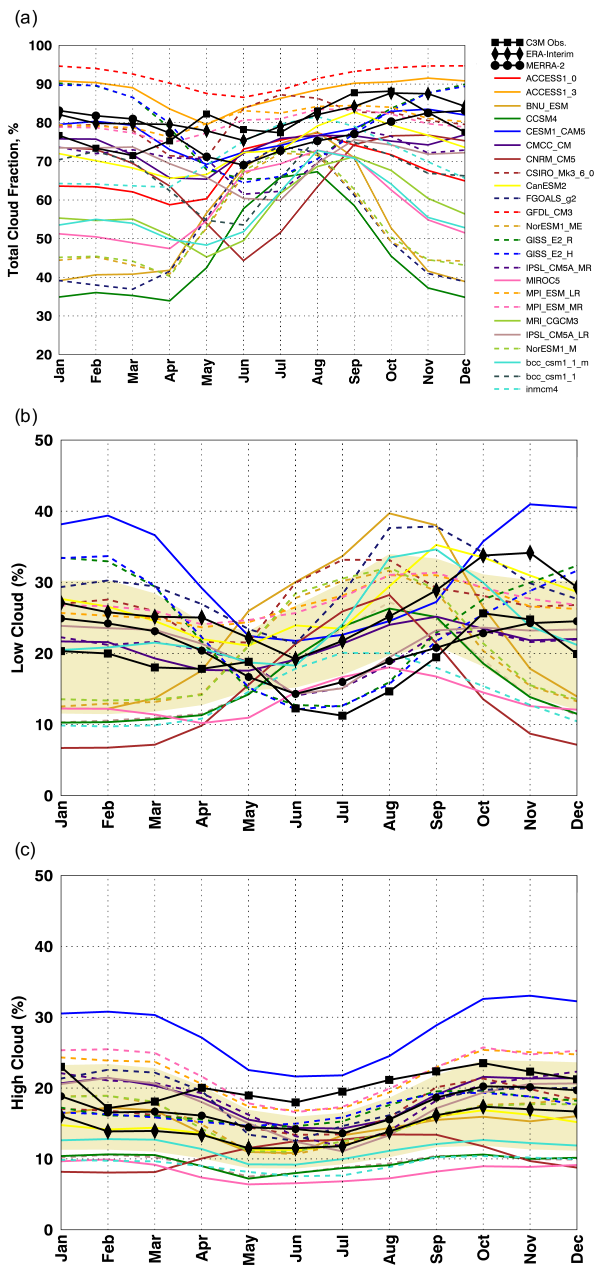
(a)
Total Cloud Fraction, %
C3M Obs.
ERA-Interim
MERRA-2
ACCESS1_0
ACCESS1_3
BNU_ESM
CCSM4
CESM1_CAM5
CMCC_CM
CNRM_CM5
CSIRO_Mk3_6_0
CanESM2
FGOALS_g2
GFDL_CM3
NorESM1_ME
GISS_E2_R
GISS_E2_H
IPSL_CM5A_MR
MIROC5
MPI_ESM_LR
MPI_ESM_MR
MRI_CGCM3
IPSL_CM5A_LR
NorESM1_M
bcc_csm1_1_m
bcc_csm1_1
inmcm4
Jan Feb Mar Apr May Jun Jul Aug Sep Oct Nov Dec
(b)
Low Cloud (%)
Jan Feb Mar Apr May Jun Jul Aug Sep Oct Nov Dec
(c)
High Cloud (%)
Jan Feb Mar Apr May Jun Jul Aug Sep Oct Nov Dec

954

Fig. 1. Annual cycle of (a) total cloud amount, (b) low cloud amount (defined as cloud between 1000 – 850 hPa) and (c) high cloud amount (cloud between 500 – 300 hPa). Colored lines represent individual CMIP5 models, black lines with symbols represent observations and reanalysis. The gray shading in (a) represents the 95% confidence interval for the difference in means between C3M and the ensemble; the yellow shading in (b)-(c) represents the ensemble mean +/- one standard deviation.

**Deleted:** Fig. 1. Annual cycle of (a) total cloud amount, (b) low cloud amount (defined as cloud between 1000 – 850 hPa) and (c) high cloud amount (cloud between 500 – 300 hPa). Color lines represent individual CMIP5 models. The black line with squares represents C3M observations and the black line with circles represents MERRA-2. The gray shading in (a) represents the 95% confidence interval for the difference in means between C3M and the ensemble; the yellow shading in (b)-(c) represents the ensemble mean +/- one standard deviation.

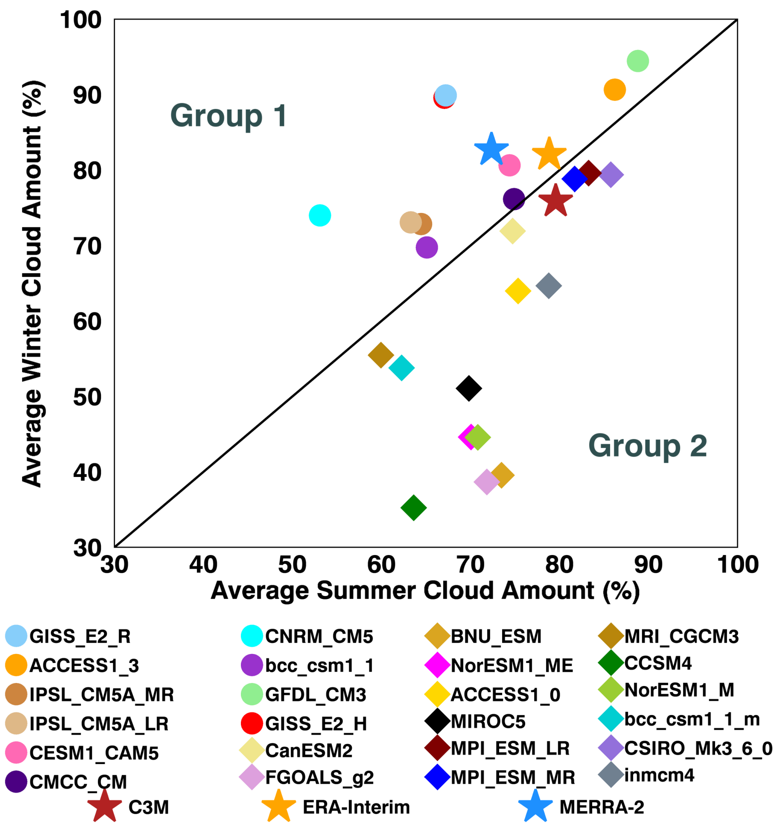


Fig. 2: Average winter (DJF) cloud fraction vs average summer (JJA) cloud fraction. Models above the 1:1 line (maximum cloud fraction in winter; circle symbols) are defined as Group 1 and those below the 1:1 line (maximum CA in summer; square symbols) are Group 2. The star symbols represent C3M observations (red) and ERA-Interim and MERRA-2 reanalysis (orange, blue).

**Deleted:** *<object>*

**Deleted:** s

**Deleted:** Fig. 2: Average winter (DJF) cloud fraction vs average summer (JJA) total cloud amount. Models above the 1:1 line (maximum cloud amount in winter; circle symbols) are defined as Group 1 and those below the 1:1 line (maximum cloud amount in summer; square symbols) are Group 2. The yellow star represents C3M observations.

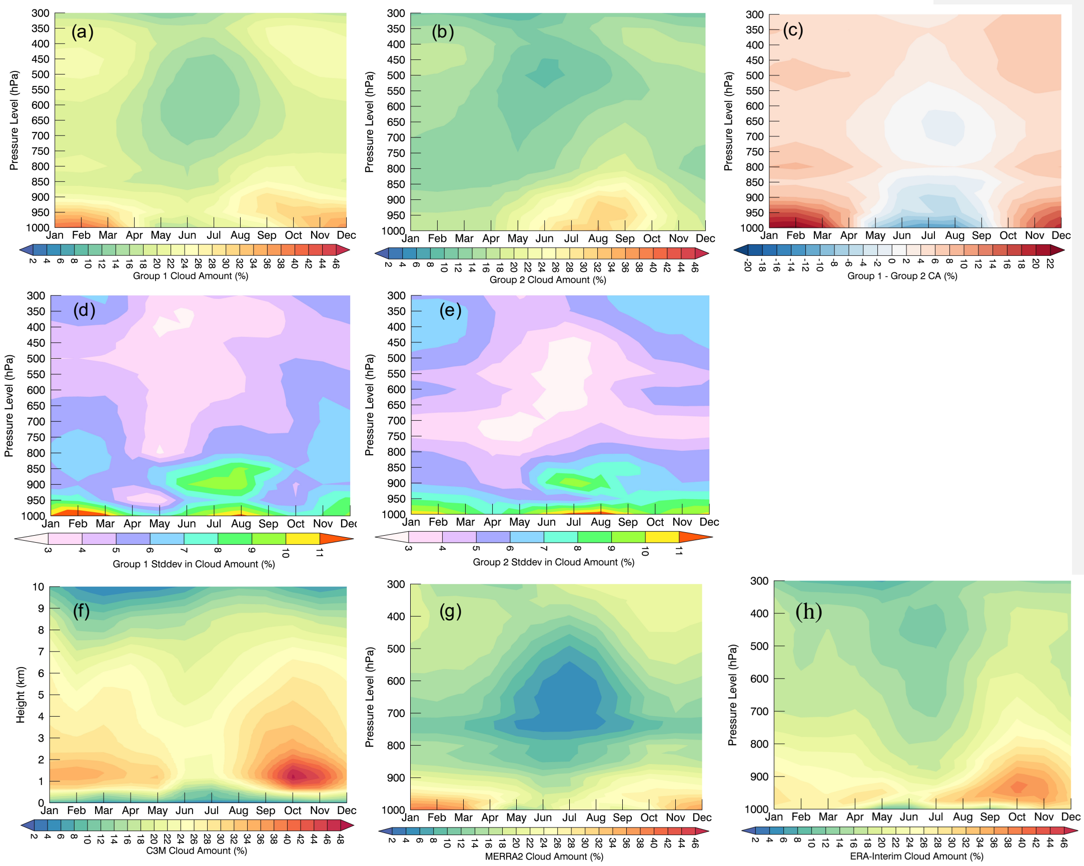


Fig. 3. Vertically-resolved mean cloud amount annual cycle for (a) Group 1, (b) Group 2, and (c) Group 1 – Group 2. The vertically resolved standard deviation across the (d) Group 1 and (e) Group 2 model members. Observational profiles of cloud amount are shown in (f) for C3M, (g) for MERRA-2 reanalysis, and (h) for ERA-Interim reanalysis.

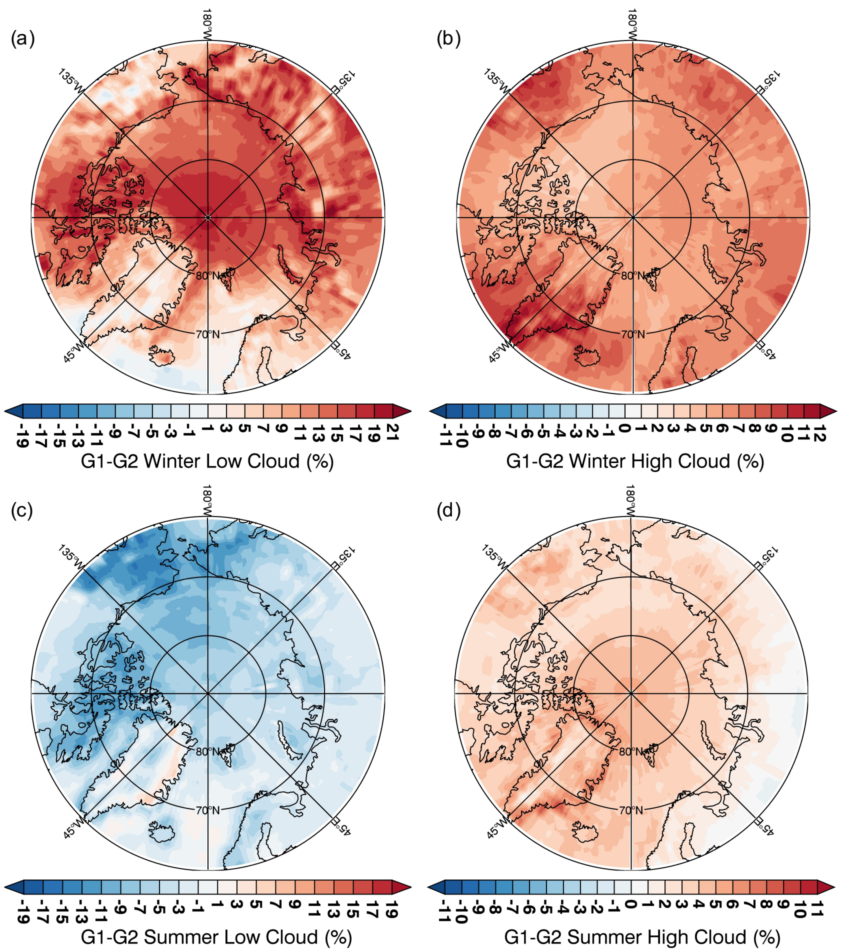


Fig. 4. Spatial variations in Group 1 minus Group 2 cloud amount differences for (a) winter low clouds, (b) winter high clouds, (c) summer low clouds, and (d) summer high clouds.

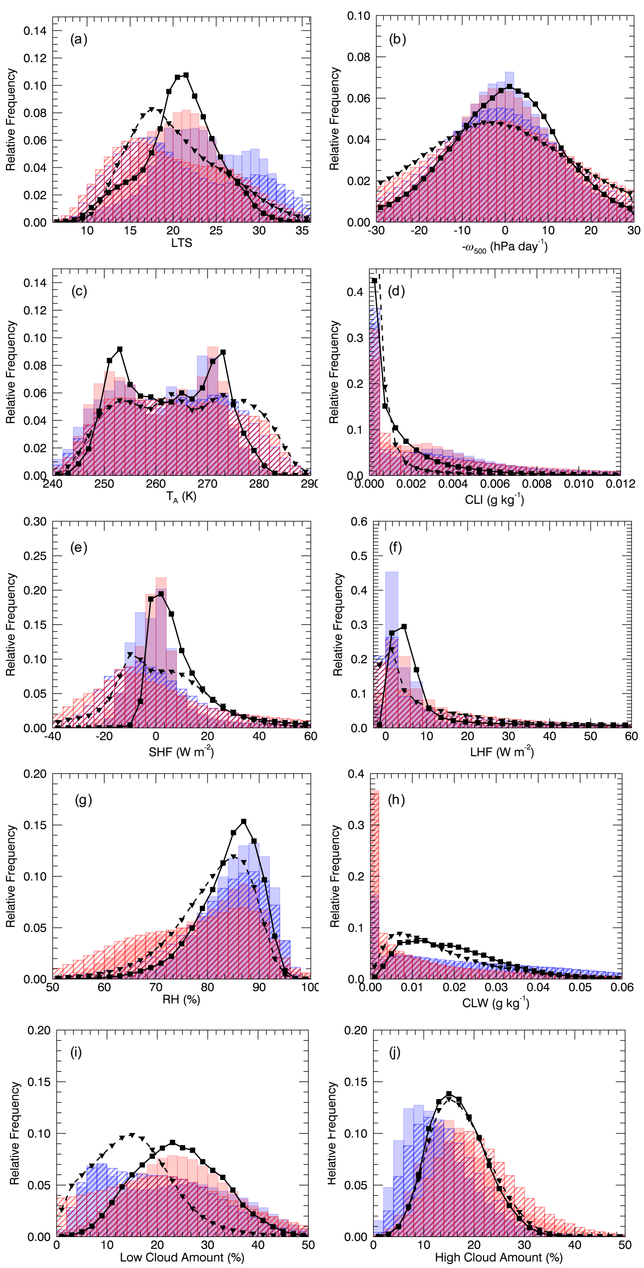


**Deleted:** ***<object>***

Fig. 5. Probability distributions of (a) LTS, (b) $-\omega_{500}$, (c) Low-Level $T_A$, (d) CLI, (e) SHF, (f) LHF, (g) RH, (h) CLW, (i) low cloud amount, and (j) high cloud amount. Red shading denotes Group 1, blue denotes Group 2, solid fill represents ocean grid boxes, and cross-hatching represents land grid boxes. The solid black line shows MERRA-2 reanalysis values for ocean (square symbol) and land (triangle symbol). Distributions are for all months of the year.

**Deleted:** ¶

**Deleted:** Fig. 5. Probability distributions of (a) LTS, (b) $-\omega_{500}$, (c) low-level $T_A$, (d) CLI, (e) SHF, (f) LHF, (g) RH, and (h) CLW. Red shading denotes Group 1, blue denotes Group 2, solid fill represents ocean grid boxes, and cross-hatching represents land grid boxes. The solid black line shows MERRA-2 reanalysis values for ocean (square symbol) and land (triangle symbol). Distributions include all months of the year.

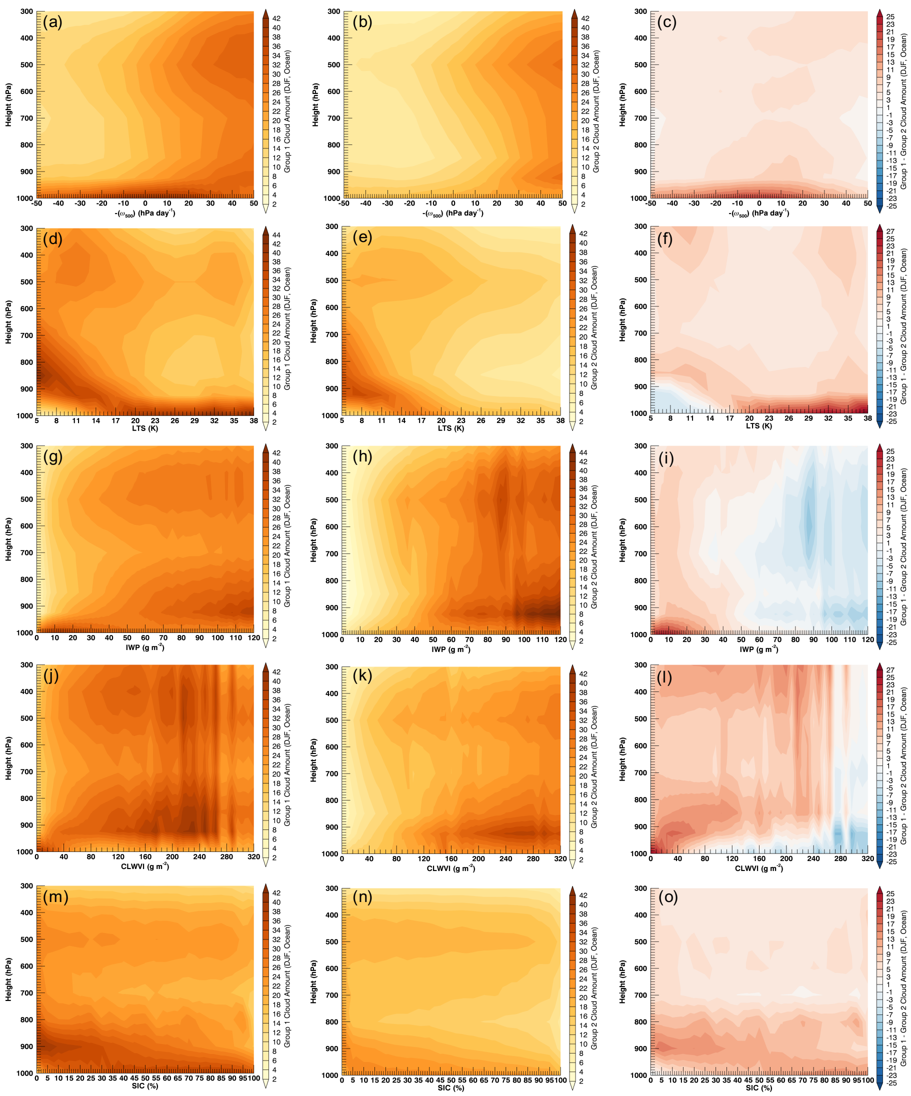


Fig. 6. Vertically-resolved, DJF average cloud amount stratified by $-\omega_{500}$ for (a) Group 1, (b) Group 2, and (c) Group 1 minus Group 2, LTS for (d) Group 1, (e) Group 2, and (f) Group 1 minus Group 2, IWP for (g) Group 1, (h) Group 2, and (i) Group 1 minus Group 2; CLWVI for (j) Group 1, (k) Group 2, and (l) Group 1 minus Group 2, and SIC for (m) Group 1, (n) Group 2, and (o) Group 1 minus Group 2. All panels are for ocean.

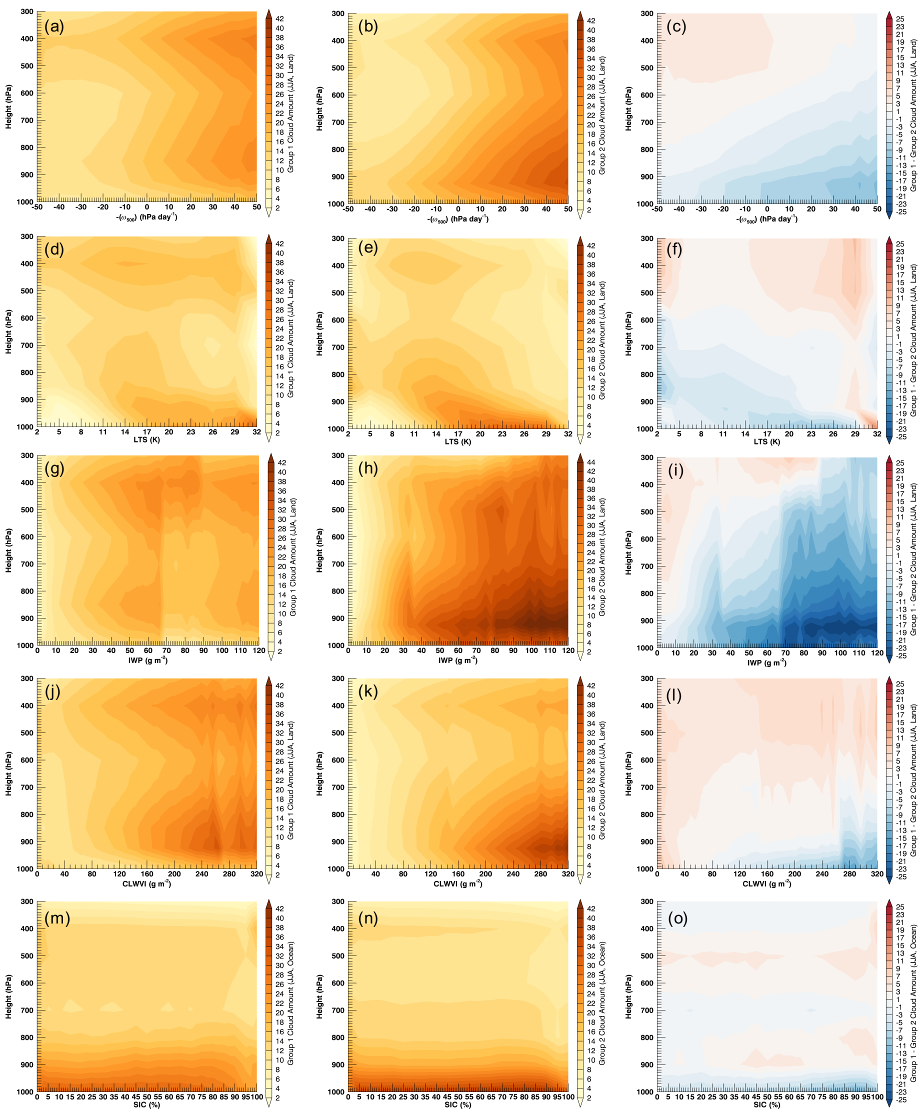


Fig. 7. Vertically-resolved, JJA cloud amount stratified by -$\omega_{500}$ for (a) Group 1, (b) Group 2, and (c) Group 1 minus Group 2, LTS for (d) Group 1, (e) Group 2, and (f) Group 1 minus Group 2, IWP for (g) Group 1, (h) Group 2, and (i) Group 1 minus Group 2; CLWVI for (j) Group 1, (k) Group 2, and (l) Group 1 minus Group 2, and SIC for (m) Group 1, (n) Group 2, and (o) Group 1 minus Group 2. All panels are over land except for SIC.

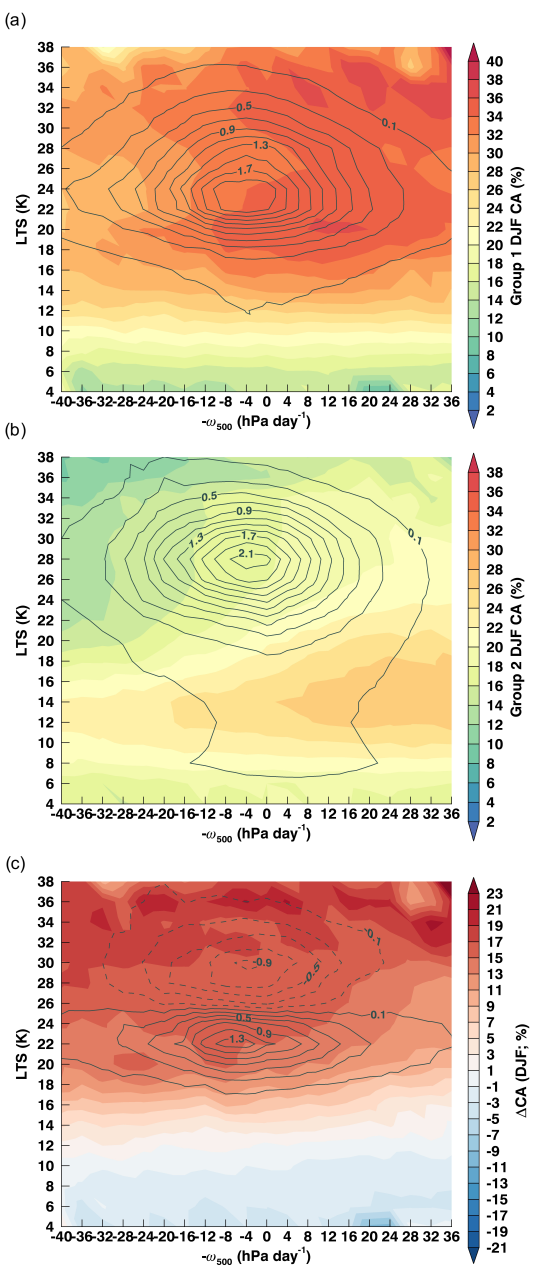
(a)
LTS (K)
-ω500 (hPa day-1)
Group 1 DJF CA (%)
(b)
LTS (K)
-ω500 (hPa day-1)
Group 2 DJF CA (%)
(c)
LTS (K)
-ω500 (hPa day-1)
ΔCA (DJF; %)

Fig. 8. Contours of average low cloud amount for winter in a *LTS*/-$\omega_{500}$ joint distribution for (a) Group 1, (b) Group 2, and (c) Group 1 minus Group 2. The frequency of occurrence each *LTS*/-$\omega_{500}$ interval is contoured in black for Group 1 (a), Group 2 (b), and the difference in frequency of occurrence (c). In (c), the solid contouring represents regimes occurring more frequently in Group 1 while the dashed contouring are those regimes occurring more frequently in Group 2.

**Deleted:** Fig. 8. Contours of average low cloud amount for DJF in the LTS and -$\omega_{500}$ joint distribution for (a) Group 1, (b) Group 2, and (c) Group 1 minus Group 2 and the frequency of occurrence each LTS and -$\omega_{500}$ interval for (d) Group 1, (e) Group 2, and (f) Group 1 minus Group 2.

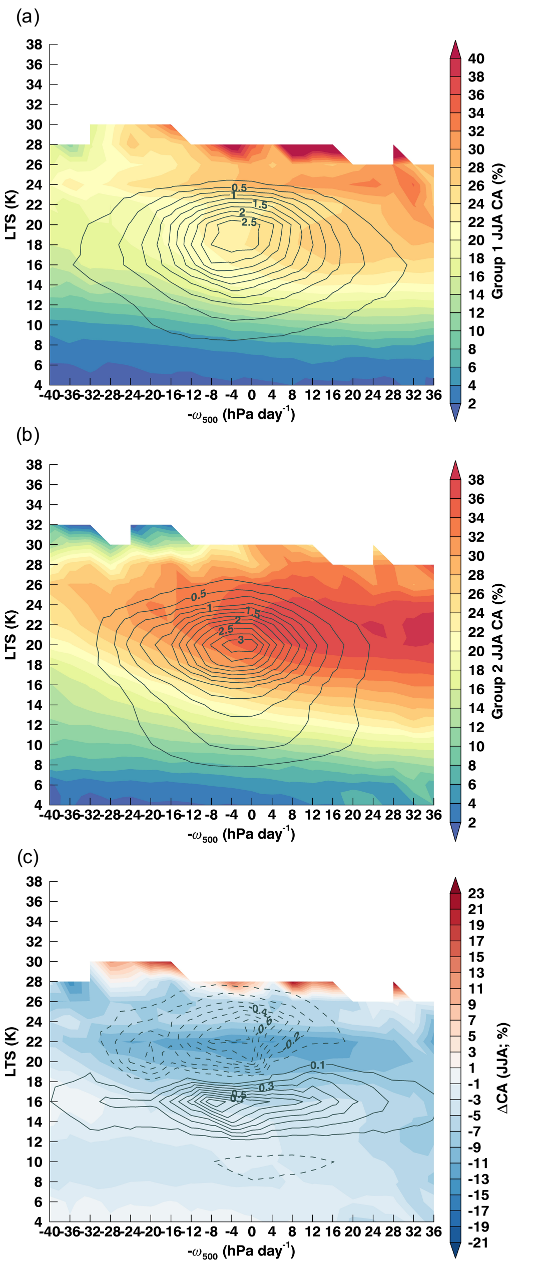
(a)
LTS (K)
-ω500 (hPa day-1)
Group 1 JJA CA (%)
(b)
LTS (K)
-ω500 (hPa day-1)
Group 2 JJA CA (%)
(c)
LTS (K)
-ω500 (hPa day-1)
ΔCA (JJA; %)

Fig. 9. Contours of average low cloud amount for summer in a *LTS*/-$\omega_{500}$ joint distribution for (a) Group 1, (b) Group 2, and (c) Group 1 minus Group 2. The frequency of occurrence each *LTS*/-$\omega_{500}$ interval is contoured in solid black for Group 1 (a), Group 2 (b), and the difference in frequency of occurrence (c).

**Deleted:** Fig. 9. Contours of average low cloud amount for JJA in the LTS and -$\omega_{500}$ joint distribution for (a) Group 1, (b) Group 2, and (c) Group 1 minus Group 2 and the frequency of occurrence each LTS and -$\omega_{500}$ interval for (d) Group 1, (e) Group 2, and (f) Group 1 minus Group 2.

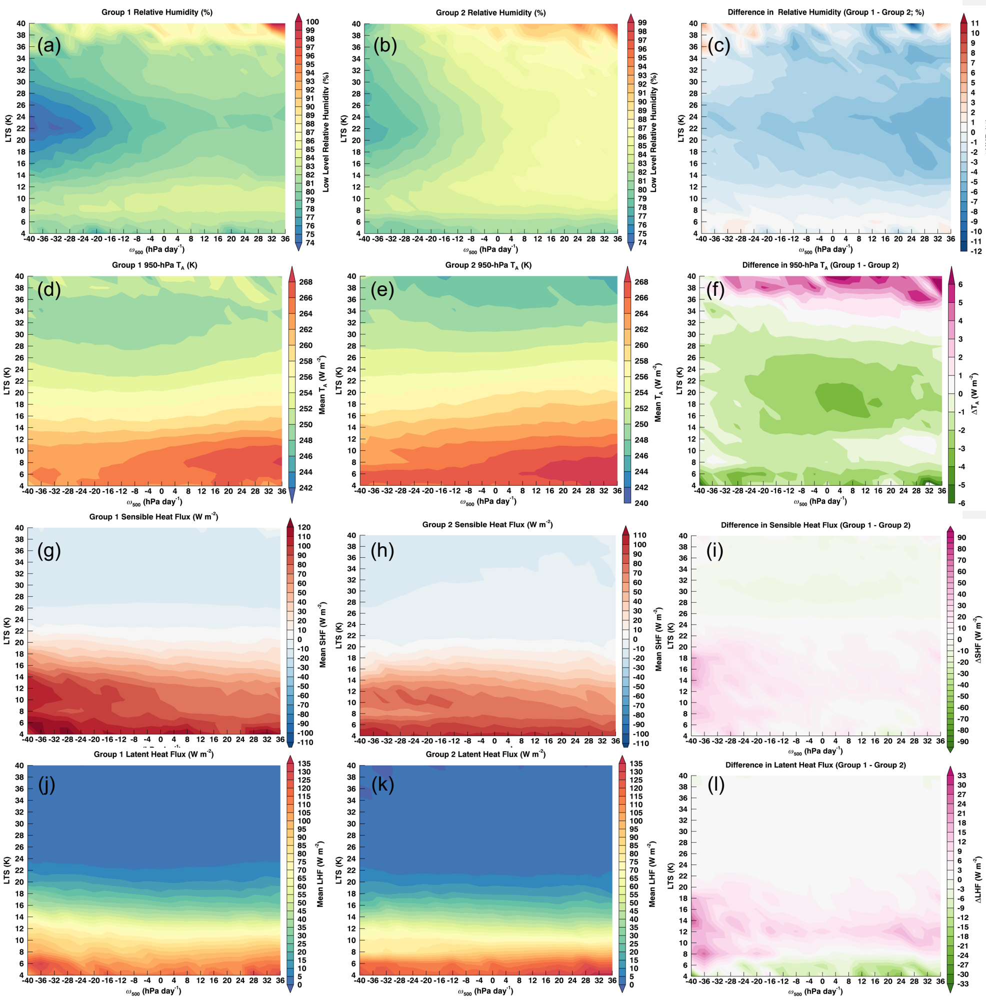


Fig. 10. Contours of DJF atmospheric and surface conditions in the LTS and -$\omega_{500}$ joint distribution for (left column) Group 1, (middle column) Group 2, and (right column) Group 1 minus Group 2 for (a-c) RH, (d-f) $T_A$ at 950hPa, (g-l) SHF, and (j-l) LHF.

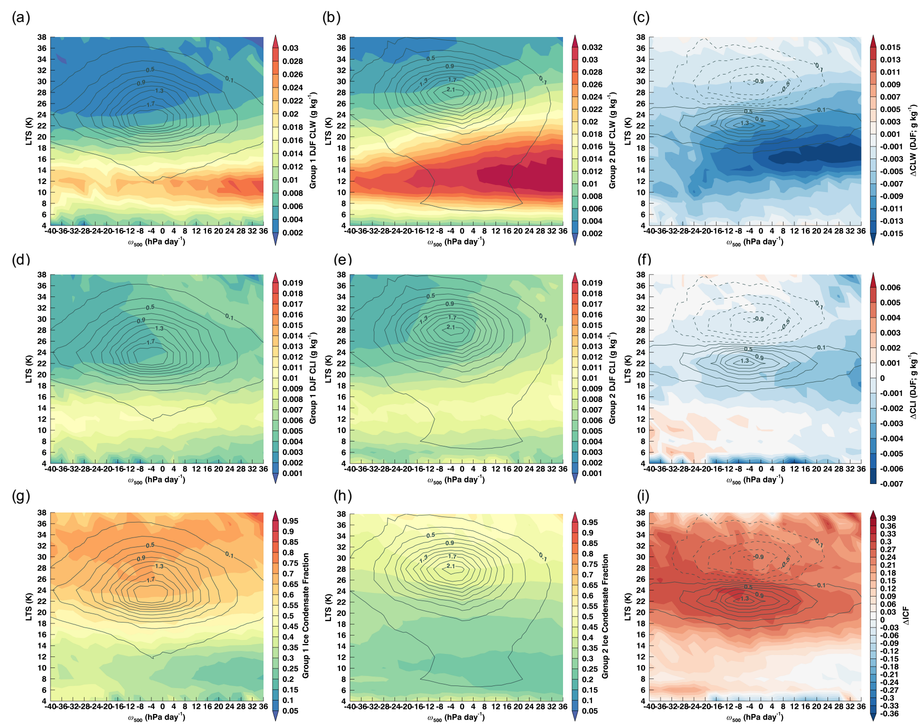


Fig. 11. Contours of winter low cloud liquid water mixing ratio for (a) Group 1, (b) Group 2, and (c) Group 1 minus Group 2 and low cloud ice water mixing ratio (d) Group 1, (e) Group 2, and (f) Group 1 minus Group 2. Ice condensate fraction is shown in the bottom panels for Group 1 (g), Group 2 (h), and Group 1 minus Group 2 (i).

**Deleted:** Fig. 11. Contours of DJF low cloud CLW for (a) Group 1, (b) Group 2, and (c) Group 1 minus Group 2 and CLI (d) Group 1, (e) Group 2, and (f) Group 1 minus Group 2.¶

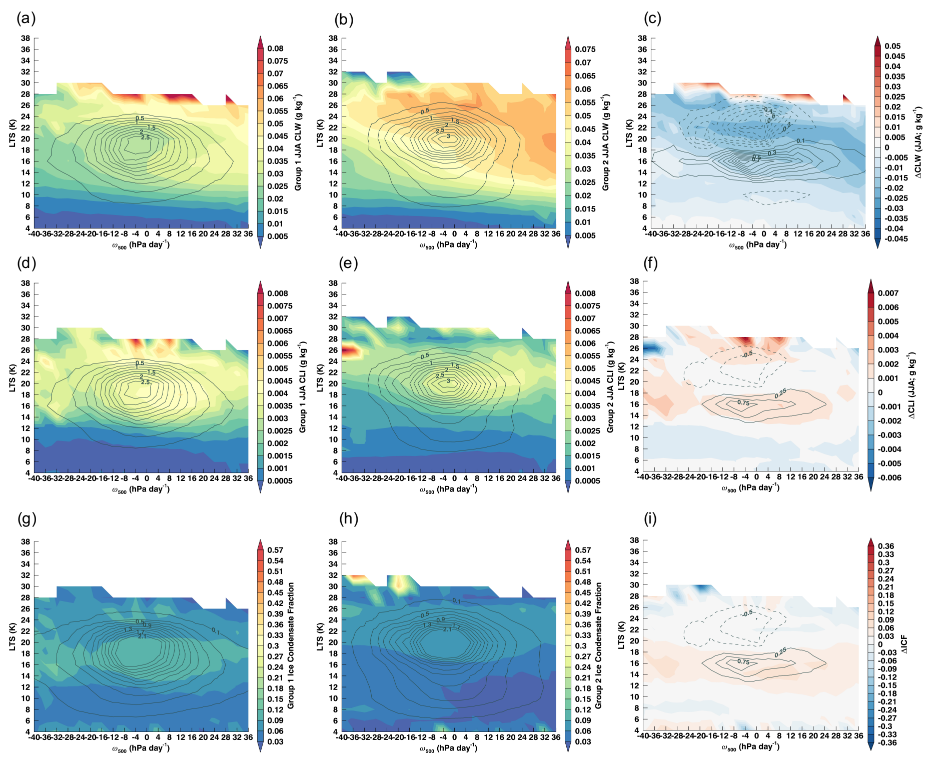


Fig. 12. Contours of summer low cloud liquid water mixing ratio for (a) Group 1, (b) Group 2, and (c) Group 1 minus Group 2 and low cloud ice water mixing ratio (d) Group 1, (e) Group 2, and (f) Group 1 minus Group 2. Ice condensate fraction is shown in the bottom panels for Group 1 (g), Group 2 (h), and Group 1 minus Group 2 (i).

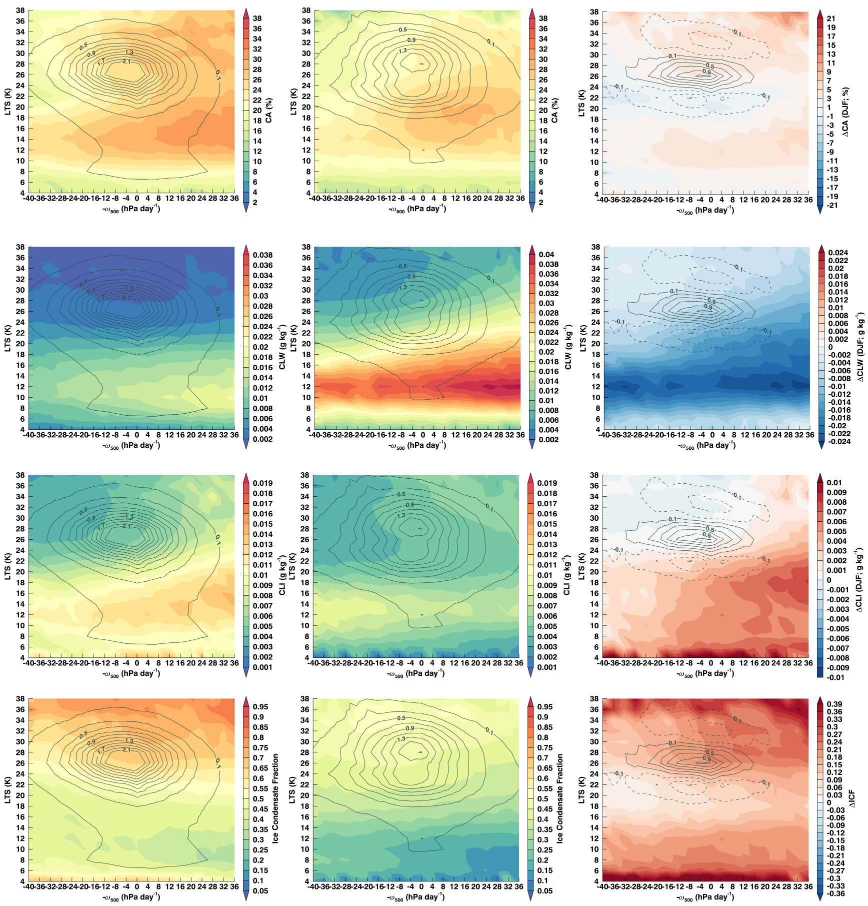


Fig. 13. Contours of winter low cloud amount for (a) Group A, (b) Group B, and (c) Group A minus Group B, low liquid water mixing ratio (d) Group A, (e) Group B, and (f) Group A minus Group B, low cloud ice water mixing ratio Group A (g), Group B (h), and Group A minus Group B (i). and ice condensate fraction is shown in the bottom panels for Group A (j), Group B (k), and Group A minus Group B (l).

**Deleted:** Fig. 12. Contours of JJA low cloud CLW for (a) Group 1, (b) Group 2, and (c) Group 1 minus Group 2 and CLI (d) Group 1, (e) Group 2, and (f) Group 1 minus Group 2.

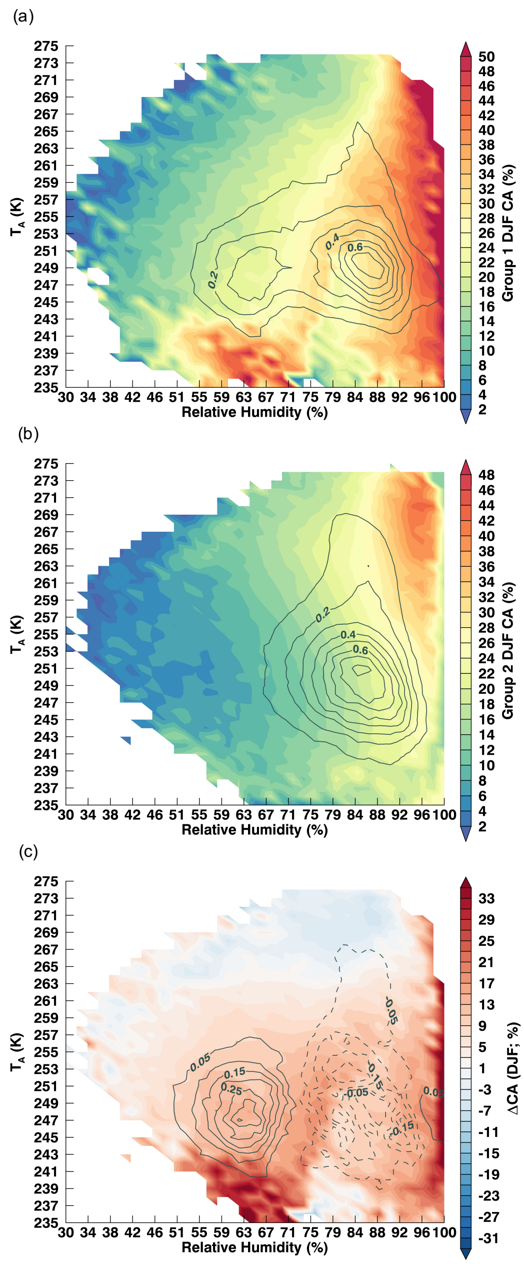
(a)
$T_A$ (K)
Relative Humidity (%)
Group 1 DJF CA (%)
(b)
$T_A$ (K)
Relative Humidity (%)
Group 2 DJF CA (%)
(c)
$T_A$ (K)
Relative Humidity (%)
ΔCA (DJF; %)

Fig. 14. Contours of average low cloud amount for winter in a $T_A$-$RH$ joint distribution for (a) Group 1, (b) Group 2, and (c) Group 1 minus Group 2. The frequency of occurrence each $T_A$-$RH$ interval is contoured in black for Group 1 (a), Group 2 (b), and the difference in frequency of occurrence (c).

**Deleted:** 3

**Deleted:** Fig. 13. Contours of average low cloud amount for DJF the TA-RH joint distribution for (a) Group 1, (b) Group 2, and (c) Group 1 minus Group 2 and the frequency of occurrence of each TA-RH interval for (d) Group 1, (e) Group 2, and (f) Group 1 minus Group 2.

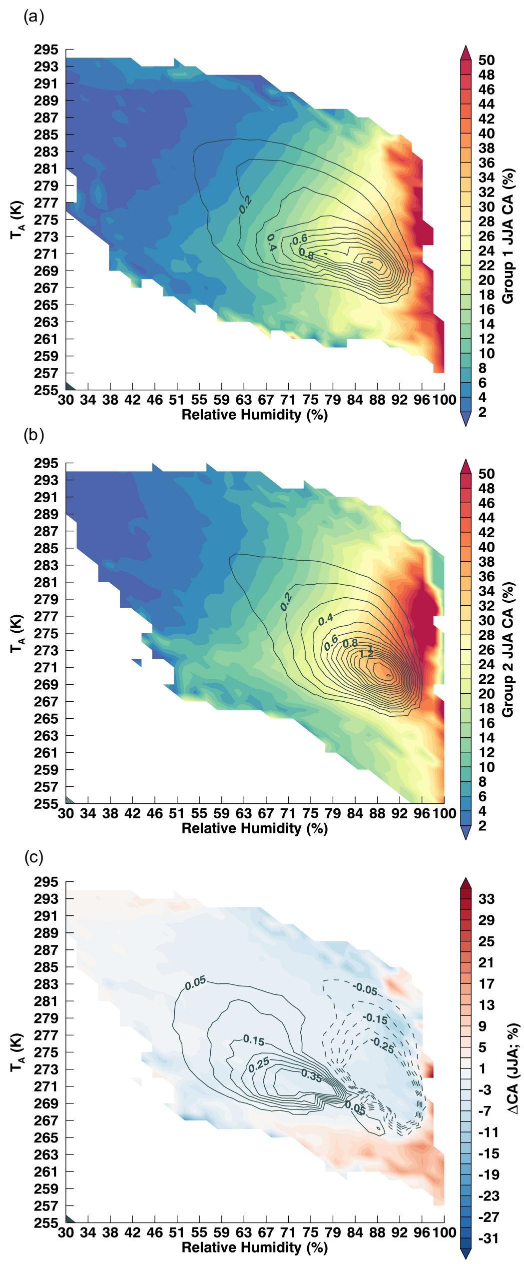
(a)
$T_A$ (K)
Relative Humidity (%)
Group 1 JJA CA (%)
(b)
$T_A$ (K)
Relative Humidity (%)
Group 2 JJA CA (%)
(c)
$T_A$ (K)
Relative Humidity (%)
ΔCA (JJA; %)

Fig. 15. Contours of average low cloud amount for summer in a $T_A$-*RH* joint distribution for (a) Group 1, (b) Group 2, and (c) Group 1 minus Group 2. The frequency of occurrence each $T_A$-*RH* interval is contoured in black for Group 1 (a), Group 2 (b), and the difference in frequency of occurrence (c).

**Deleted:** 4

**Deleted:** Fig. 14. Contours of average low cloud amount for JJA the TA-RH joint distribution for (a) Group 1, (b) Group 2, and (c) Group 1 minus Group 2 and the frequency of occurrence of each TA-RH interval for (d) Group 1, (e) Group 2, and (f) Group 1 minus Group 2.

| | | |
|---|---|---|
| **Page 30: [1] Deleted** | **Robyn Boeke** | **3/19/19 1:53:00 PM** |

| | | |
|---|---|---|
| **Page 30: [2] Deleted** | **Robyn Boeke** | **3/19/19 1:53:00 PM** |

| | | |
|---|---|---|
| **Page 30: [3] Deleted** | **Robyn Boeke** | **3/19/19 1:54:00 PM** |

| | | |
|---|---|---|
| **Page 30: [4] Deleted** | **Robyn Boeke** | **3/19/19 1:54:00 PM** |